RESULTS & DISCUSSIONS

Preformulation study:

HPLC analytical & bioanalytical method development & validation:

The calibration curves of the drugs (PTX & Gen) and their combination (PTX+ Gen) were made by using methanol (for in vitro samples) & plasma (for in vivo samples) as solvents which followed linearity from 500-3000 ng/ml for in vitro samples & 1000-5000 ng/ml for in vivo for all samples. The R^2 values are given in Table 5.1. (58)

Table 5.1: Correlation Coefficient (R^2) Values of PTX, Gen and their combination

Samples	(Correlation Coefficient) R^2 Values			
	PTX	Gen	Combination	
			PTX	Gen
In vitro	0.976	0.971	0.994	0.986
In vivo	0.971	0.976	0.973	0.986

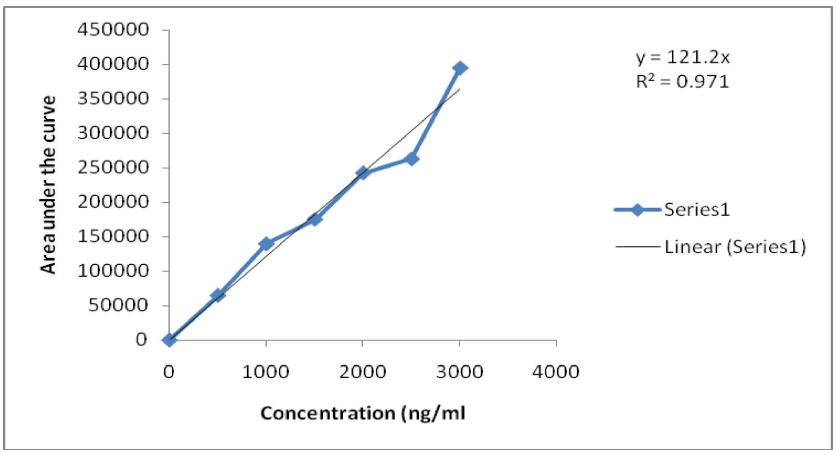

Figure 5.1: Calibration curve of Genistein in methanol

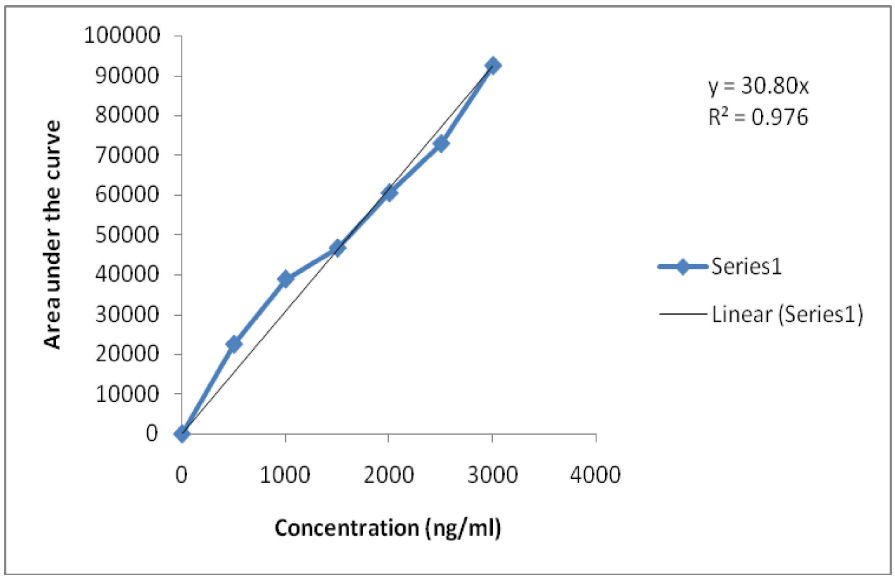

Figure 5.2: Calibration curve of Paclitaxel in methanol

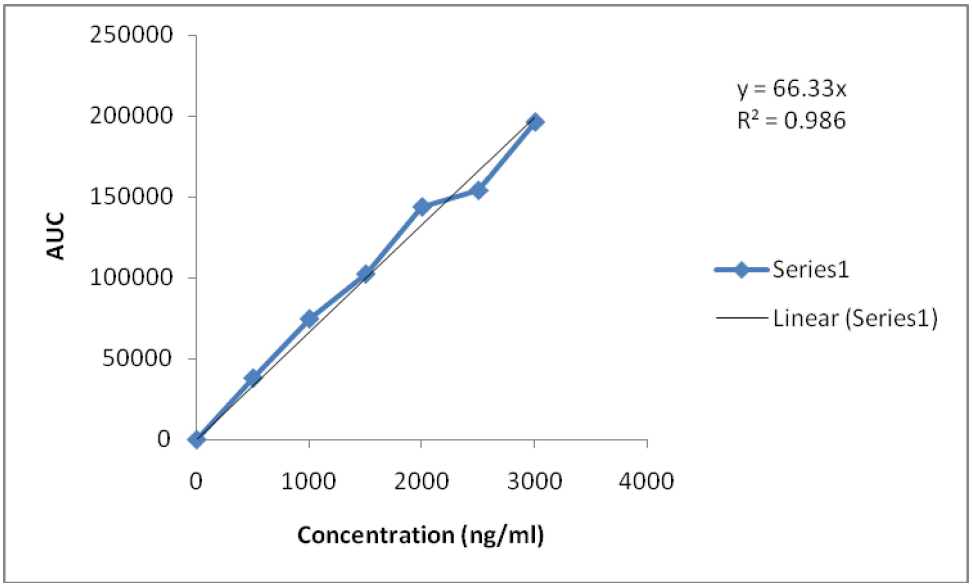

Figure 5.3: Calibration curve of Genistein in combination of Gen & PTX prepared in methanol

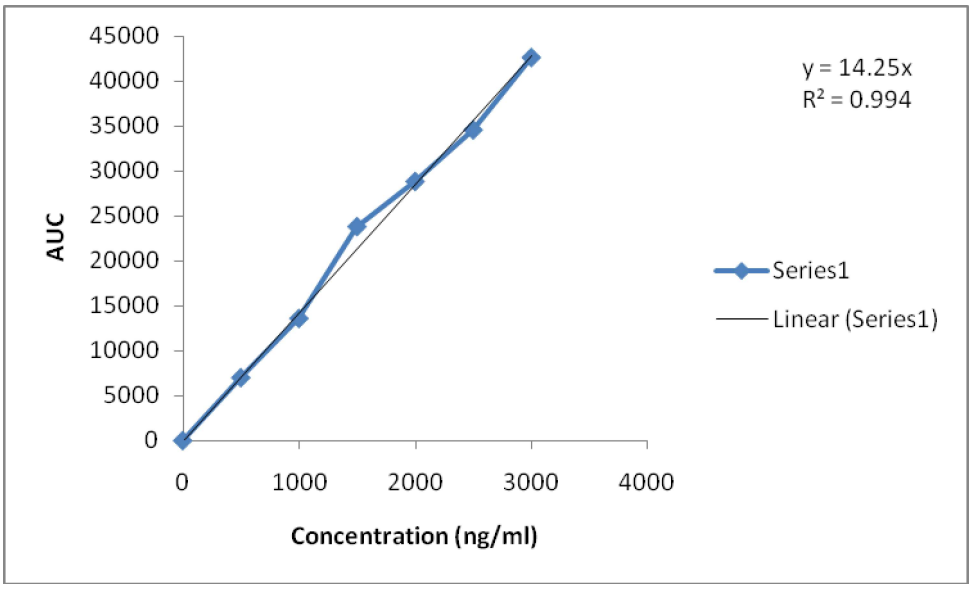

Figure 5.4: Calibration curve of Paclitaxel in combination of Gen & PTX prepared in methanol

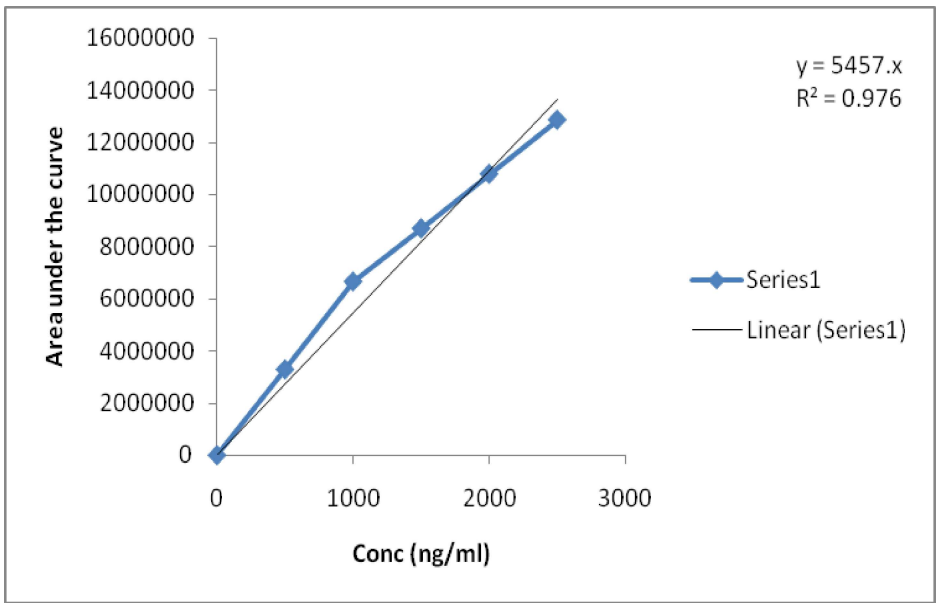

Figure 5.5: Calibration curve of Genistein in plasma

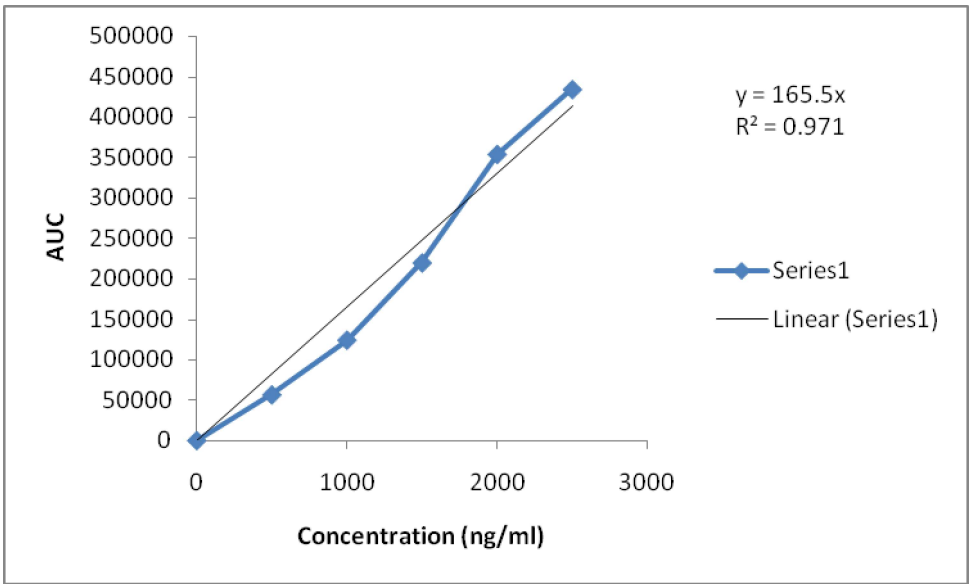

Figure 5.6: Calibration curve of Paclitaxel in plasma

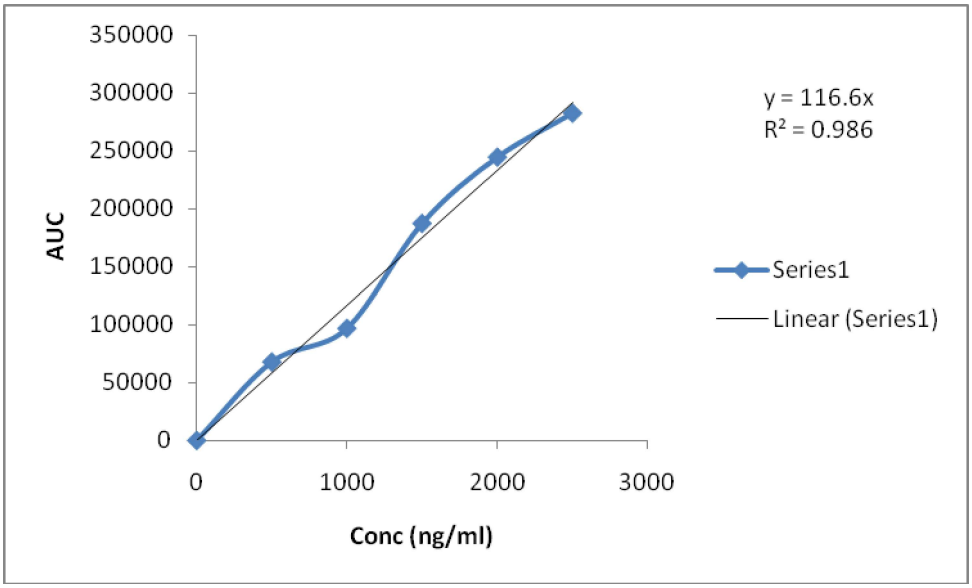

Figure 5.7: Calibration curve of Genistein in combination of Gen & PTX prepared in plasma

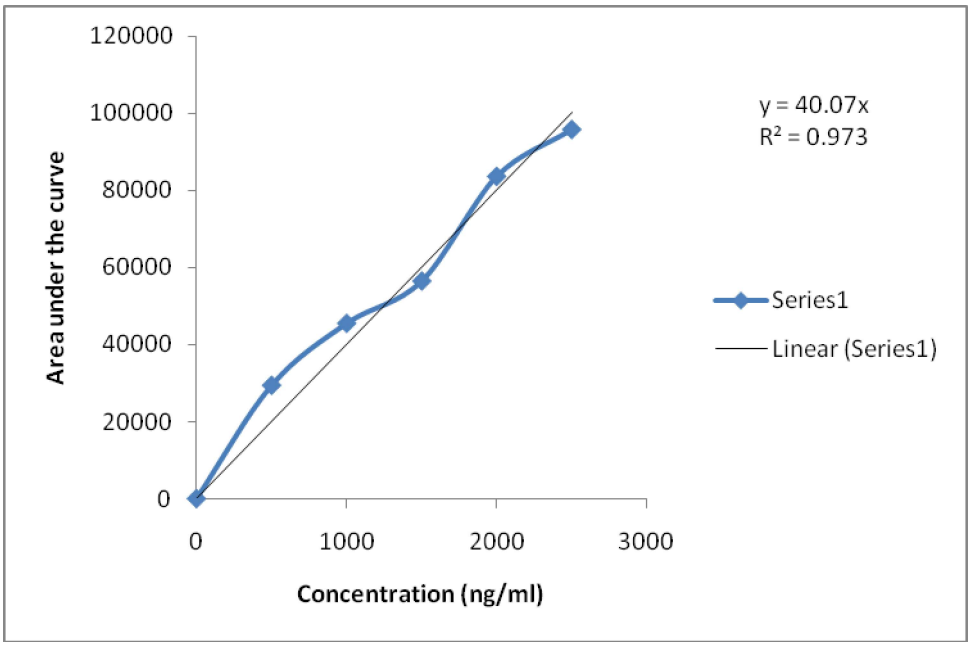

Figure 5.8: Calibration curve of Paclitaxel in combination of Gen & PTX prepared in plasma

Range & Linearity:

Six point calibration curves were constructed for Gen, PTX & Gen+PTX in the concentration range 500-3000 ng/ml and regression parameters like slope, intercept and correlation coefficient of these plots were determined as shown in Table 5.1 and calibration curves are given in Figure 5.1-5.8. The values of correlation coefficients confirmed their suitability for the further analysis.

Table 5.2: HPLC validation parameters for the determination of pure drugs (Gen & PTX) and their combination in methanol

Parameters	PTX	Gen	Combination	
			PTX	Gen
Wavelength (λ_{max}) (nm)	227	262	227	262
Retention Time (RT) (min.)	4.2	1.3	4.0	1.2

Slope	30.80	121.2	14.25	66.33
LOD (ng/ml)	389	410	427	330
LOQ (ng/ml)	529	550	537	570
Range (ng/ml)	500-3000	500-3000	500-3000	500-3000

Table 5.3: HPLC validation parameters for the determination of pure drugs (Gen & PTX) and their combination in plasma

Parameters	**PTX**	**Gen**	**Combination**	
			PTX	**Gen**
Wavelength (λ_{max}) (nm)	227	262	227	262
Retention Time (RT) (min.)	4.3	1.2	4.0	1.4
Slope	165.5	5457	40.07	116.6
LOD (ng/ml)	487	420	432	350
LOQ (ng/ml)	519	520	547	560
Range (ng/ml)	500-3000	500-3000	500-3000	500-3000

Accuracy & Precision:

It was calculated by analyzing standard samples at 3 different concentrations in triplicate within the calibration range. The experimental values are shown in Table 5.4 & 5.5. The accuracy (% recovery) of the method was found to be 100±5% indicating the fair agreement between true and obtained values. The inter and intraday precision values showed % RSD values to be <3% indicating repeatability and intermediate precision of the developed method.

Table 5.4: Inter and Intraday accuracy and precision for analytical method validation by HPLC

Concentration (ng/ml)	Accuracy		Precision	
	Intraday	**Inter day**	**Intraday**	**Inter day**
		Genistein		
1500	102.44±1.43	100.43±1.176	1.89	2.11
2000	101.87±1.52	103.22±2.01	1.67	1.81
2500	100.56±1.12	102.87±1.98	1.62	2.01
		Paclitaxel		
1500	99.22±1.87	98.23±2.12	2.33	1.98
2000	101.28±2.11	100.98±1.90	2.12	2.11
2500	102.94±1.198	103.22±2.111	2.70	2.50
		Gen in combination		
1500	102.76±2.11	102.98±2.95	2.10	1.70
2000	101.79±1.56	101.91±1.93	1.82	1.92
2500	100.57±2.27	100.98±1.63	1.40	1.39
		PTX in combination		
1500	99.43±2.11	100.67±1.09	2.11	1.93
2000	98.63±1.89	99.11±2.1	2.53	2.67
2500	100.24±1.4	100.11±2.3	2.51	2.87

Table 5.5: Inter and Intraday accuracy and precision for bioanalytical method validation by HPLC

Concentration (ng/ml)	Accuracy		Precision	
	Intraday	Inter day	Intraday	Inter day
		Genistein		
1500	103.24±1.66	101.22±1.12	2.11	2.36
2000	101.24±1.76	102.09±1.21	1.54	1.10
2500	99.86±2.25	101.03±1.92	1.73	1.98
		Paclitaxel		
1500	100.02±1.65	99.06±2.82	2.18	1.89
2000	102.13±2.12	103.18±1.10	1.87	1.51
2500	103.14±1.14	101.12±2.86	1.83	1.05
		Gen in combination		
1500	100.46±1.71	101.46±2.25	3.01	2.71
2000	98.79±1.56	99.21±1.93	1.87	1.12
2500	100.12±2.35	101.18±2.63	3.10	1.09
		PTX in combination		
1500	99.03±3.22	101.17±1.3	1.99	1.92
2000	100.23±1.21	101.35±2.15	2.52	1.37
2500	103.14±1.56	101.61±2.45	2.87	3.12

Specificity and sensitivity:

For the drug sample analysis, the peaks of the drug should be specific without interference of other peaks and developed method should be sensitive enough to determine the lower concentration of the drug in the samples. Specificity of the method was determined by injection of dosage forms. No interfering peaks of the excipients were observed at their respective RTs which indicate that the developed method was

specific enough. To determine the sensitivity, LOD (Limit of detection) and LOQ (limit of quantification) were determined based on the method of slope of standard curve and standard deviation (SD) of response.

LOD= 3.3 SD/Slope

LOQ= 10 SD/Slope

Synergism analysis of ratiometric drug combination:

The effect of Gen combined with PTX on cell viability was observed using MTT assay. For this study, PA-1 (human epithelial ovarian cancer cells) were treated with Gen combined with PTX in ratios of 1:10, 1:5, 1:1, 5:1 &10:1 and analyzed for cytotoxicity at different F_a values (fraction affected) (0.1-0.9). CI was calculated from data points with F_a >0.5 by using Compusyn® (Biosoft, Ferguson, MO, USA) software. Treatment at different ratios resulted in decrease in cell viability which was greater than alone drug. To indicate the effect at different F_a values, the CI (combination index) and DRI (dose reduction index) values were calculated at each F_a (Figure 5.9). DRI > 1 represents chances of reduction of dose in the combination. CI <1 was observed at F_a > 0.6, corresponds to most synergistic effect. In our study, higher doses of PTX with smaller doses of Gen (1:1, 5:1 and 10:1) showed maximum synergism and 5:1 (PTX:Gen) combination was selected for further studies,

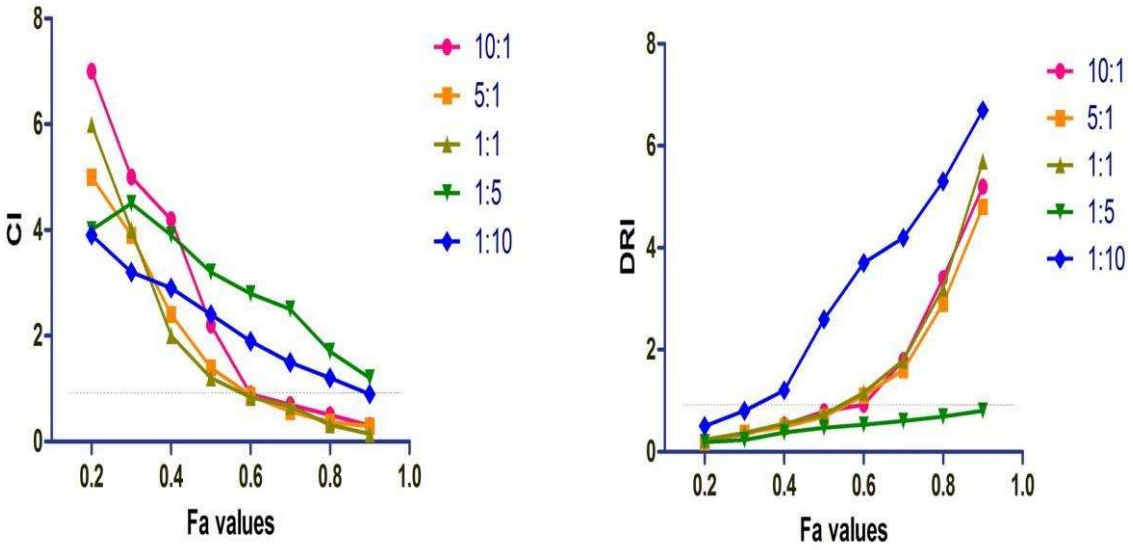

Figure 5.9: CI and DRI plots for different F_a values

Result & Discussion of Nanostructured lipid carriers:

Optimization of process and product Parameters for Blank NLCs

Table 5.6: Quality Target Product Profile (QTPP)

QTPP Elements	Target	Justification
Dosage form	Nanostructured lipid carriers (NLCs)	Lipid based systems that help in enhancing the bioavailability of the poorly water soluble drug and nano systems helps in targeting the drug to the particular area in case of cancer.
Dosage design	Delayed release	Decreases dosage frequency as well as toxicity caused by drugs.
Administration route	Intravenous	Required to target the drug to the cancerous area.
Finished product	Lyophilized powder	It will be stable and easy for packaging.
Stability	Minimum 08 months	To maintain the therapeutic potential of the drug.

Table 5.7: Control Impact Matrix

CONTROL	IMPACT		
Critical quality attributes (CQAs)	**High**	**Medium**	**Low**
In our Control	➢ Type of raw materials (oils, solid lipids, surfactants etc. ➢ Concentration of lipids, surfactants ➢ Type of water/organic solvent used ➢ Amount of Water phase/ organic phase ➢ Speed of magnetic stirrer /homogenizer/sonicator ➢ Time of homogenization ➢ Method of preparation ➢ Injection speed ➢ Needle size used ➢ Temperature of the system	➢ Efficiency of formulator	**---------**
Out of Control	➢ Purity of raw materials ➢ Partition coefficient of the drug ➢ Solubility profile of drug ➢ Efficiency of measurement system ➢ Environmental conditions (Room temperature, humidity, pressure etc)	➢ Efficiency of Analyst, Chemist.	Contamination

Table 5.8: Critical Process parameters and material attributes

Sr. No	CPPs	CMAs
1.	Method of preparation used	Type of Liquid lipid, solid lipids & surfactants
2.	Speed of magnetic stirrer/homogenizer/sonicator	Concentration of SL, LL & surfactant used
3.	Time of homogenization/ sonication	Type of water/ organic solvent used
4.	Injection Speed	Ration of Aqueous phase/ organic phase
5.	Temperature of the system	Needle size
6.	Efficiency of measurement system	

Table 5.9: Risk Estimation Matrix

CTQ (CMAS+ CPPs)	Particle Size	Poly dispersity Index	Entrapment Efficiency
Type of lipids used	High	Low	High
Amount of lipids	High	Medium	High
Type of surfactant	High	Low	Low
Surfactant conc.	High	High	Medium
Solvent type	High	Low	Medium
Humidity	Low	Low	Low
Solvent ratio	High	Low	High
Temperature of the system	High	Low	High
Speed of homogenizer	High	Medium	Medium
Homogenization time	High	Low	High
Sonication time	High	Medium	Low
Stirring speed	Medium	Low	Medium

Type of Analyst	Low	Low	Low
Stirring time	High	Low	Low
Injection Speed	High	Medium	Low
Needle Size	Medium	Low	Low
Method of preparation	High	Low	Medium
Room Temperature	Low	Low	Low

The Placket Burman design (PBD):

Total 20 no. of experimental runs were generated from 12 factors at 2 levels PB design with 3 responses (Table no. 5.10). It was found that particle size was mostly influenced by the brand of lipid, a brand of surfactant and lipid concentration. The factors influencing the entrapment efficiency were found to be the brand of lipid, a brand of surfactant and surfactant concentration whereas for Polydispersity index, the significantly affecting factors were the brand of lipid, a brand of surfactant and organic solvent concentration (Fig.5.10) ($p<0.05$). As per our data, we analyzed the fact that different brand of the same lipid and different brand of the same surfactant are the two parameters which significantly affects all the three responses. We had solved our problem by manually using all the 4 combinations of surfactant and lipid brand and then characterized the formulation for all 3 responses mentioned above and finalized the brands of both lipid and surfactant. From our observations, we noted that best results of all 3 responses were obtained when we used Sigma Aldrich based Tristearin as lipid and Sigma Aldrich based TPGS vitamin E as a surfactant. Further, the three remaining parameters, i.e., lipid concentration (affecting particle size), surfactant concentration (affecting entrapment efficiency) & organic solvent concentration (affecting polydispersity index) were chosen as variables for further response surface methodology.

Table 5.10: Details of factors used for Placket Burman design

Codes	Independent Variables	Low level (-1)	High Level (+1)	Unit	Type of factor
A.	Brand of the same lipid	TCI Chemicals	Sigma Aldrich	-	Category
B.	Brand of the same surfactant	Antares	Sigma Aldrich	-	Category
C.	Injection Speed	5	10	ml/min	Numeric
D.	Height of the syringe	2	5	cm.	Numeric
E.	Speed of magnetic stirrer	900	1200	Rpm	Numeric
F.	Time of magnetic stirring	4	8	Min.	Numeric
G.	Homogenization time	10	15	Min.	Numeric
H.	Homogenization Speed	12500	15000	Rpm	Numeric
I.	Ultrasonication Time	4	8	Min.	Numeric
J.	Lipid Concentration	0.75	1.0	% w/v	Numeric
K.	Surfactant Concentration	0.1	0.3	% w/v	Numeric
L.	Amount of Organic solvent	5	10	Ml	Numeric

Dependent Variables
Particle Size (nm)
Poly dispersity index
Entrapment efficiency (%)

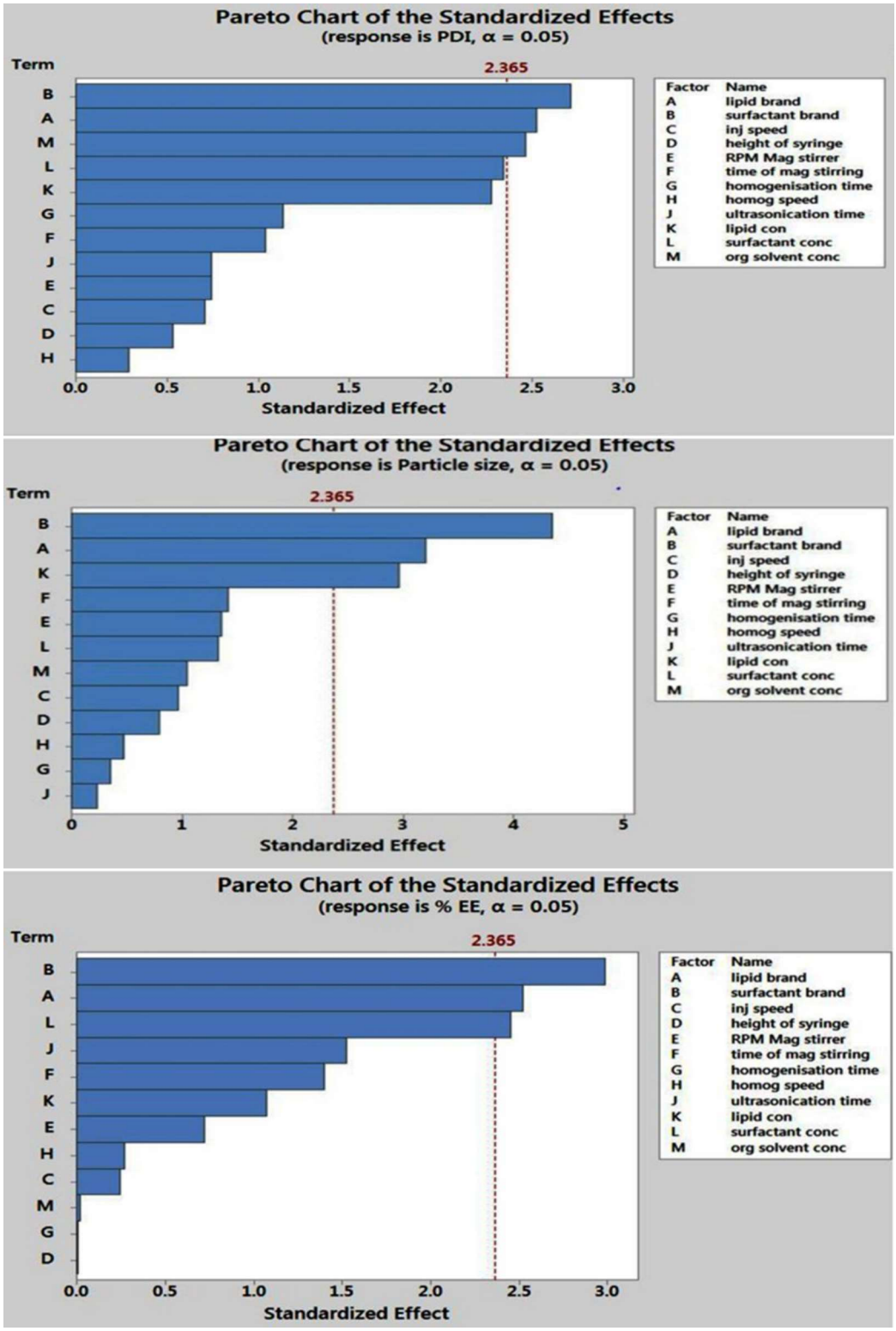

Figure 5.10: Pareto chart showing the influence of process variables on polydispersity index, particle size & entrapment efficiency

The Box-Behnken design (BBD): The response surface methodology:

Influence of variables on particle size:

The formulations were prepared by varying the drug for each experimental run randomly but all the other parameters were kept same as that stated by experimental design. The particle size of NLCs varied from 123.3 nm to 389.3 nm for various level combinations of all factors in the design matrix. The F value of 228.26 shows that model allows acceptable fitting of data with non significant lack of fit (3.06). Moreover, a p-value of <0.0001 suggests that this is the best-fitted model for this particular response. The low value of the coefficient of variation (2.58) also reveals some important facts that model posses‟ high degree of precision and reliability. The "Pred R-Squared" of 0.9636 is in reasonable agreement with the "Adj R-Squared" of 0.9927. Therefore, we can use this response to navigate the design space. The results of the statistical analysis were represented in Table 5.11.

It was discovered from the results of statistical analysis (Figure 5.11) that both surfactant concentration (X1) & amount of organic solvent (X3) affects the particle size negatively while lipid concentration has positive effect on the same, i.e., if we go on decreasing the surfactant concentration and amount of solvent, particle size of the nanoformulation will increase while it will increase with increase in lipid content. Here, the concentration of surfactant (X1) appears to be strongly influencing parameter for particle size owing to its effect on the emulsification ability which defines the particle size of the formulation. It possesses a negative relationship with particle size. On the contrary, a remarkable increase in particle size was seen with increased concentration of lipid concentration. It can be attributed to increase in viscosity of the contents and thereby reducing the shearing efficiency of the stirrer as well as reducing the

emulsification ability of the surfactant. In the same manner, the amount of organic solvent posses inverse relationship with particle size which can be due to a decrease in viscosity of the lipid contents with a higher amount of organic solvent, thereby imparting high shear stress which would break the emulsion droplets without any coalescence (11, 55, 59).

Table 5.11: Statistical ANOVA based results of quadratic model & the quadratic equation generated by Design Expert®

Response	Quadratic model						
	F-Value	P-Value*	R-Square	R-Sq (adj)	CV%	Lack of fit	Remark
P.Size(nm)	228.26	<0.0001	0.997	0.9927	2.58	3.06	Significant
EE (%)	66.79	<0.0001	0.9901	0.9753	1.48	1.34	Significant
PDI	26.78	<0.0004	0.957	0.9393	7.67	4.8	Significant

R-Sq (adj)= R Square adjusted; CV= Coefficient of variation

*p-value<0.05 is considered as statistically significant

*Y	Particle size (Y1)	Entrapment efficiency(Y2)	Polydispersity index (Y3)
X_0	+272.58	+85.85	+0.14
A	-104.44	+9.41	-0.052
B	+12.66	+2.63	+04.25E-003
C	-4.5	0.99	-0.023
A*B	-1.52	-4.53	+4.75E-003
A*C	-21.90	-0.35	+0.014
B*C	-0.75	+0.025	+7.75E-003
A^2	-19.87	-1.87	+0.052
B^2	-15.87	-3.10	-5.75E-003
C^2	+14.75	-0.73	+8.00E-003

*Y= response; X_0 = intercept; A-C= Factors

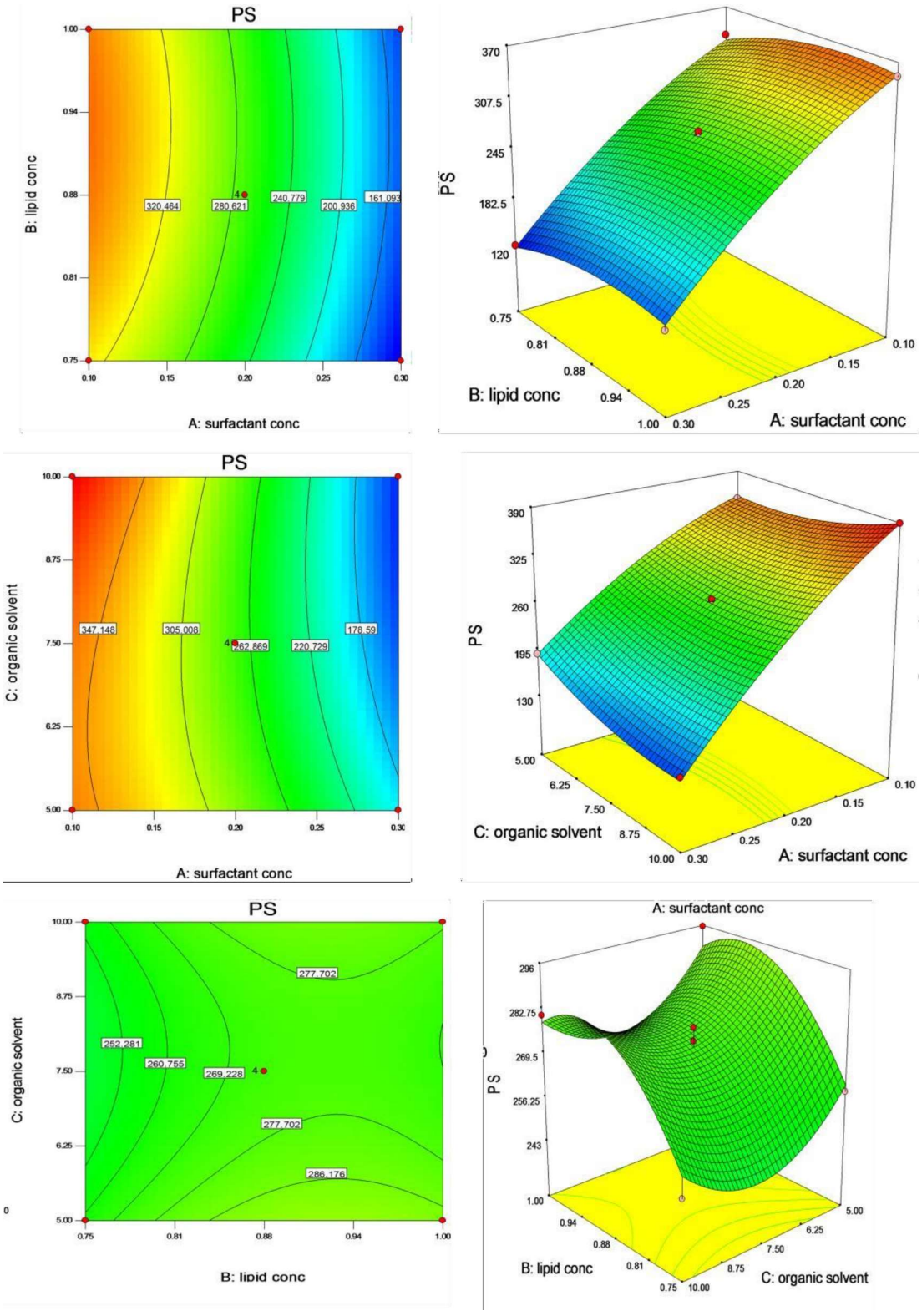

Figure 5.11: Graphical representation of effect of independent variables (lipid concentration (X1), amount of organic solvent (X2) & Surfactant concentration (X3)) on dependant variable (particles size (Y1).

Influence of variables on entrapment efficiency (EE):

To calculate the effect of variables on EE, 10 mg of both drugs and their combination was added to the formulation on randomized basis. The entrapment efficiency of NLCs varied from 63.4%- 93.4% for different formulation variable combinations. The second order polynomial equation generated by the Design Expert software equating entrapment efficiency with various factors is given in Table 5.11. The modal value of F= 66.79 ($p<0.0001$) implied that the chosen model is the right choice for relating % EE with independent factors. The suitability of the model with the excellent fitting of data was also certified by non significant lack of fit (1.34). The sufficiently high value of correlation coefficient (R^2) (0.9901) indicated the good correlation between factors and responses. The "Pred R-Squared" of 0.9047 is in reasonable agreement with the "Adj R-Squared" of 0.9753."Adeq Precision" measures the signal to noise ratio. A ratio greater than 4 is desirable. Our ratio of 30.543 indicates an adequate signal. This model can be used to navigate the design space. From Figure 5.12 , we found that surfactant concentration (X1), lipid concentration (X2) and amount of organic solvent (X3), all affect the % EE positively, i.e., increasing any of the factors will positively increase the entrapment efficiency. Increase the lipid concentration will provide the thick layer to curtail the further diffusion of the drug to the surrounding and also more lipid content will dissolve more amount of drug which will lead to increased EE (11, 59). Also, it will work only with higher surfactant and higher organic solvent amount as merely increasing the lipid concentration without any increase in organic solvent may lead to decrease in EE as sufficient amount of organic solvent is needed to dissolve the lipid, if organic solvent concentration is low, it will lead to thick foam formation in the medium and drug will remain outside. It can also be explained by change in viscosity of the

emulsion on decreasing the organic phase content. Increase in viscosity will result in higher viscous resistance against a shear force which will hinder the formation of nano droplets and also the lesser amount of drug will get solubilized into viscous lipid matrix which ultimately results into decrease entrapment efficiency (60). Similarly, sufficiently high surfactant concentration is also needed to form a particle of uniform size with good entrapment efficiency as at lower surfactant concentrations, sufficient amount of drug will not be able to dissolve in the lipid medium which will further lead to decrease in entrapment efficiency (61).

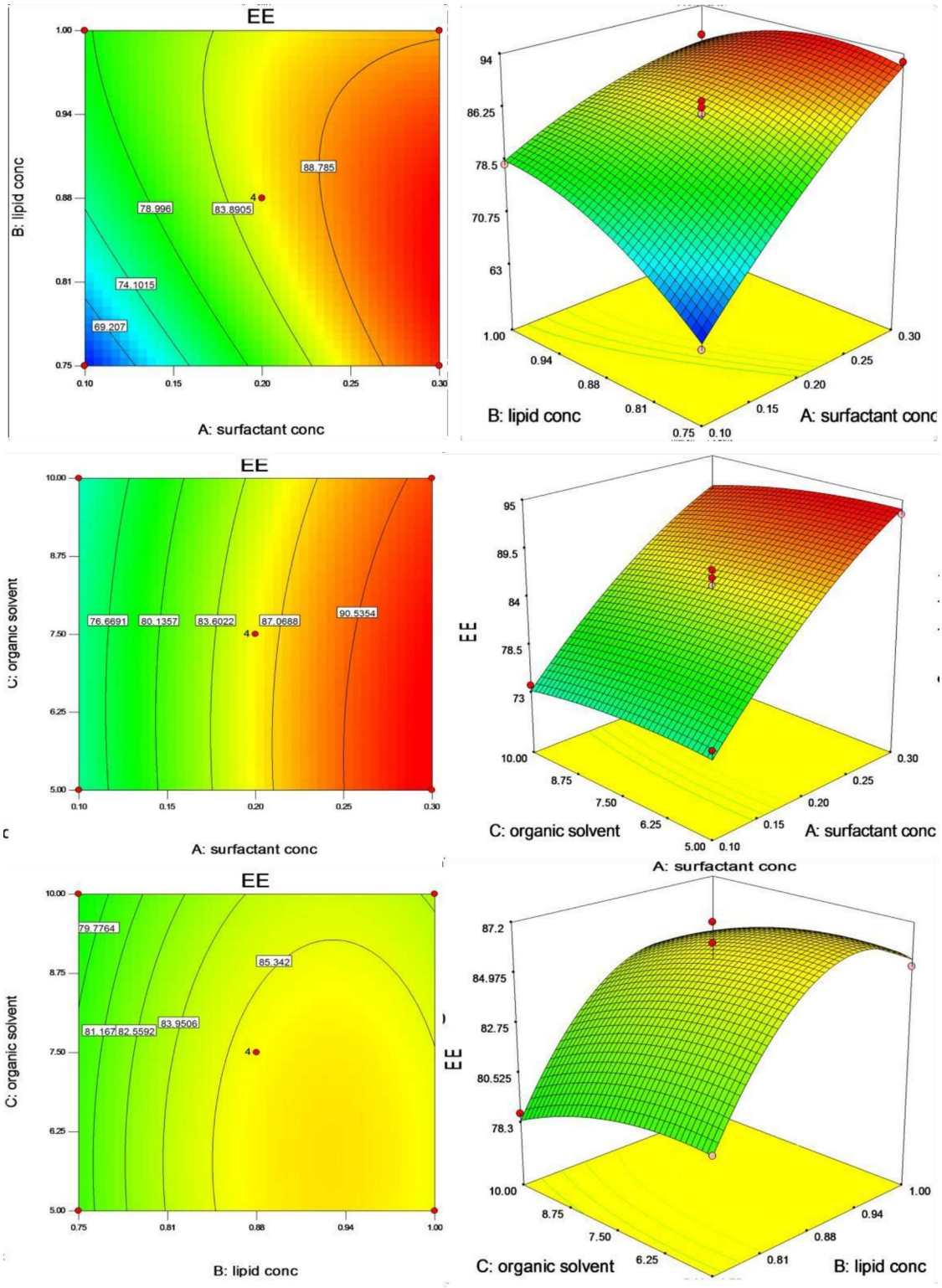

Figure 5.12: Graphical representation of effect of independent variables (lipid concentration (X1), amount of organic solvent (X2) & Surfactant concentration (X3)) on dependant variable (Entrapment Efficiency (Y2).

Influence of process variables on polydispersity index (PDI)

The value of PDI varies from 0.112-0.289 for various combinations of process parameter at their minimum and maximum levels. The second order polynomial equation generated by multiple linear regressions is given in Table 5.11. The chosen model was found to be statistically significant having good F value of 26.78 at $p<0.0001$. Moreover, the suitability and good reliability of the PDI on the chosen responses was also reflected by its nonsignificant lack of fit value (4.8). A good correlation between dependent and independent factors was justified by their sufficiently high R-square value (0.957). In this case, A, C, A^2 were significant model terms (Table 5.11). The influence of various parameters on PDI was evaluated by relating Figure 5.13, where we found that surfactant concentration (X1) & amount of organic solvent (X3) affects the response negatively while lipid concentration (X2) has its positive effect on the PDI. Increase in lipid concentration will increase the value of PDI owing to its direct impact on the thickness of formulation contents. The Higher viscosity of the lipid matrix will suppress their segregation or will promote the aggregation of the nanoparticles by suppression of their negative charge which would result in the irregular distribution of the particles and hence higher will be the PDI (11, 59, 61). Nevertheless, significant decrease in PDI was observed with increase in surfactant concentration (X1) and amount of organic solvent (X3) which can be attributed to the marked reduction in interfacial tension between aqueous and organic phase which will provide homogeneity to the particles and result in decreased PDI(11, 51, 53, 59, 62).

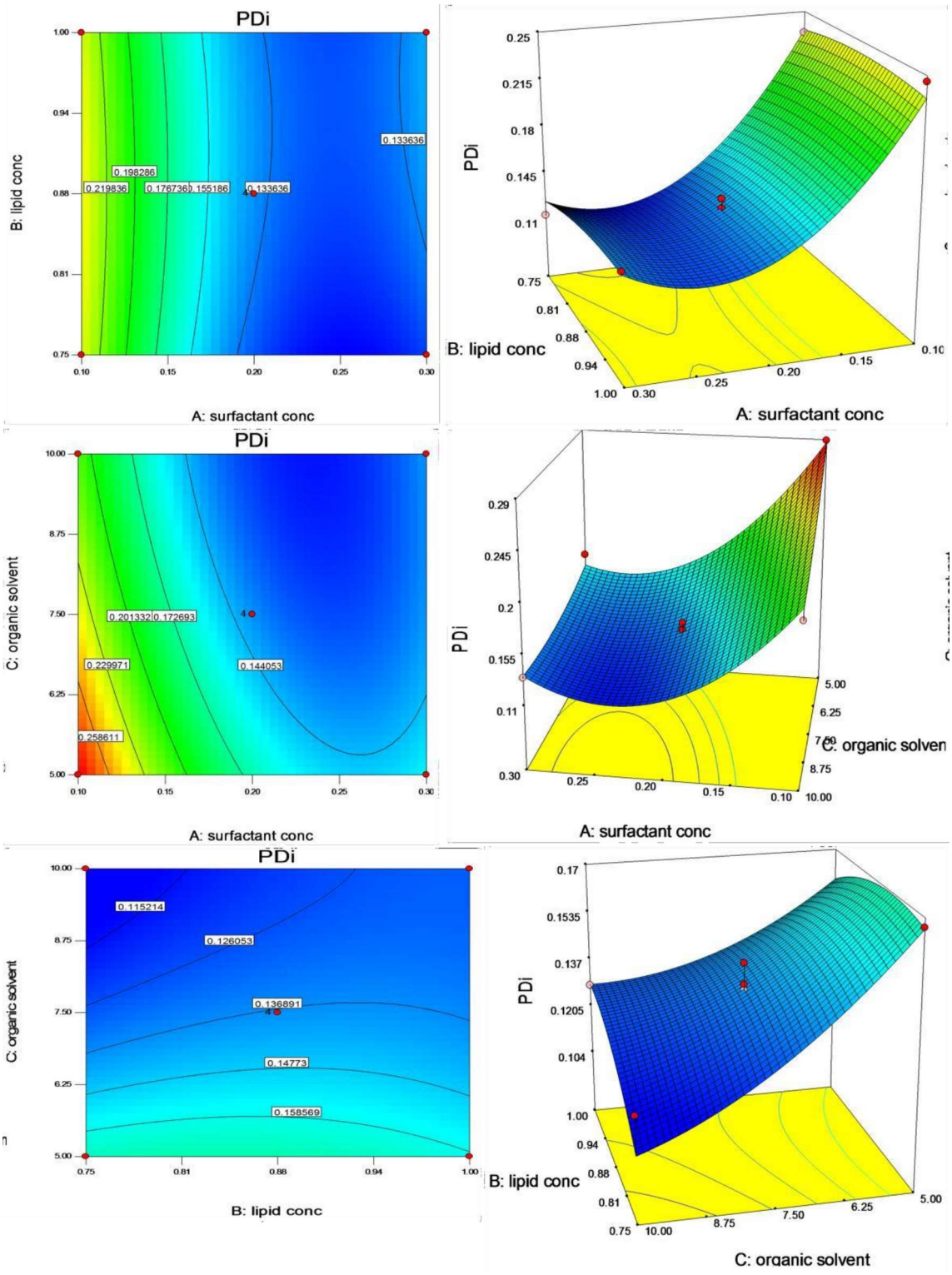

Figure 5.13: Graphical representation of effect of independent variables (lipid concentration (X1), amount of organic solvent (X2) & Surfactant concentration (X3)) on dependant variable (Polydispersity Index (Y3).

Optimization of NLCs:

Numerical optimization technique based on desirability function was used to optimize the final formulation of NLC using box Behnken methodology. Using the desirability approach, we had fixed the constraints for each variable which would result in maximum entrapment efficiency value and minimum particle size and PDI values as listed in Table 5.12. Accordingly, the optimized formulations were formulated for confirming the validity of the software. Percentage biasness was calculated between average experimental values and predicted values. Average values of all formulations were taken to evaluate the experimental values of the parameter. A good agreement between the predicted and experimental values confirmed the reliability of the response surface design for optimization of the NLC formulation.

Table 5.12: Desirability approach based numerical optimization of various factors

Independent Variables	Levels
Surfactant conc (X1)	0.3% w/v
Lipid conc (X2)	0.76% w/v
Amt of org solvent (X3)	8.31 ml

Responses	Predicted value	Experimental value	% bias[a]
Particle Size	118.20 nm	122.91 nm	-3.9%
Entrapment Efficiency	92.03%	93.29%	-1.36%
Polydispersity Index	0.120	0.115	4.16%
Overall Desirability		0.969	

All results were expressed as mean ±SD, n=3. [a]Bias is calculated as [(predicted value-experimental value) / predicted value] x 100.

Fourier Transformed Infrared studies (FTIR):

The FTIR technique was employed to study the drug excipient compatibility as well as for the identification of the drugs. The FTIR spectra of PTX, nanoparticles containing PTXNLC (A2), Gen, GenNLC (A1), combination of PTX+Gen, NLCs containing combination of both drugs,1:1 physical mixture and all the excipients are shown in figure 4 (a), (b) & (c) respectively. In Figure 5.14(A), the spectra of D2 (Gen) possesses major peaks near 1500, 1700, 3000, 3050 and 3400 cm^{-1} which corresponds to amide –NH bending, Amine C=O stretch, aromatic –CH stretch, -OH stretch and secondary –NH stretch respectively. In Figure 5.14(B), PTX (D3) exhibited peaks near 1100cm^{-1} & 1350 cm^{-1} which correspond to C-O stretch and another peak near 1350 cm^{-} and C=C stretch respectively. Two more peaks near 1680 and 1750 cm^{-1} corresponding to C=O stretch of amide and ester respectively. Further peaks near 2970 cm^{-1} , 3100 cm^{-1} ,3250 cm^{-1} & 3400 cm^{-1} were observed which may be due to aliphatic –CH- chain stretch, an aromatic stretch of –CH-, -NH- stretch and –OH- stretch respectively. The major peaks mentioned above confirms the structure of the PTX which confirms the identity of the drug. In Figure 5.14(C), the peaks of secondary –NH stretch (3412.190), aromatic C-H stretch (2962.76), C=H aliphatic stretch (2922.25), C=O keto stretch (1732.13), C=O amide stretch (1624.40) & C=O stretch (1244.13) were present which confirmed the combination of both drugs. Further, the FTIR data of optimized formulation A1, A2 & A3) had shown the absence of major peaks of drugs which confirms the encapsulation of the maximum drug inside the NLCs while they retained all the major peaks of the components used. Also, the presence of all major peaks of the components confirmed the compatibility of the excipients and the drug.

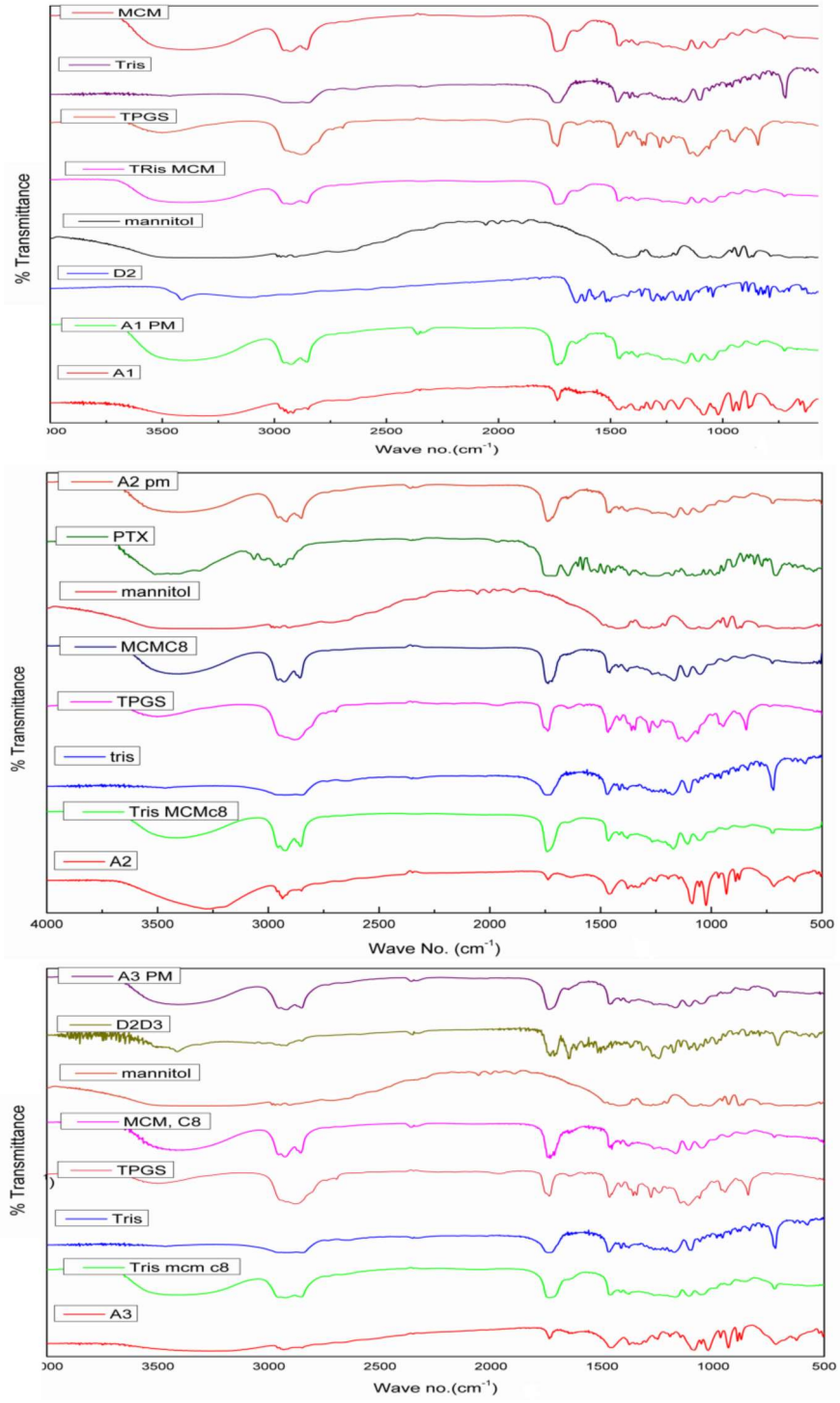

Figure 5.14: (A) Overlay FTIR spectra of Gen NLCs (A1), (B) Overlay FTIR spectra of PTXNLCs (A2), (C) Overlay FTIR spectra of combination NLCs (A3), Physical mixture (A1, A2 & A3 PM), Gen (D2),PTX (D3), Gen+ PTX (D2+D3) and all the excipients respectively.

Differential scanning calorimetery (DSC):

In DSC thermogram (Figure 5.15(A), Gen (D1) exhibit melting peak near 300˚C which is due to the actual melting of the molecule. In physical mixture (A1PM), melting peak of Gen was not visible while it contains the major peaks of surfactant (TPGS), solid lipid (Tristearin) and liquid lipid (Capmul MCM). The DSC thermo gram of PTX (D3) (Figure 5.15 (B) showed an endothermic peak near 180- 220˚C which corresponds to the melting of the compound followed by an exothermic peak near 250˚C which corresponds to the degradation of the drug molecule. The physical mixture (A2 PM) showed the absence of melting and degradation peaks of PTX while showed the major peaks due to the presence of surfactant as well as lipid mix. In Figure 5.15(C), the DSC thermogram of D2+D3 showed one endothermic peak followed by exothermic peak near 210˚C which can be due to the PTX and one endothermic peak near 280˚C followed by the exothermic peak which is due to the presence of Gen. The physical mixture (A3 PM) retained the peaks of lipid mix and surfactant. The absence of peaks of Gen and PTX in physical mixtures (A1, A2 & A3 PM) may be due to the solvation of the drugs respectively. Similarly, lyophilized formulations (A1, A2 & A3) showed the absence of major peaks of Gen & PTX whereas the sharp melting peak was present near 160˚C in all the spectra which was due to the presence of mannitol. Mannitol was added as cryoprotectant to the formulations during lyophilization. The peaks of the other excipients were present in the lyophilized formulation. The absence or reduction of peaks of drugs in the formulation can be attributed to the successful encapsulation of the drug molecule inside the nanoparticle formulations (44).

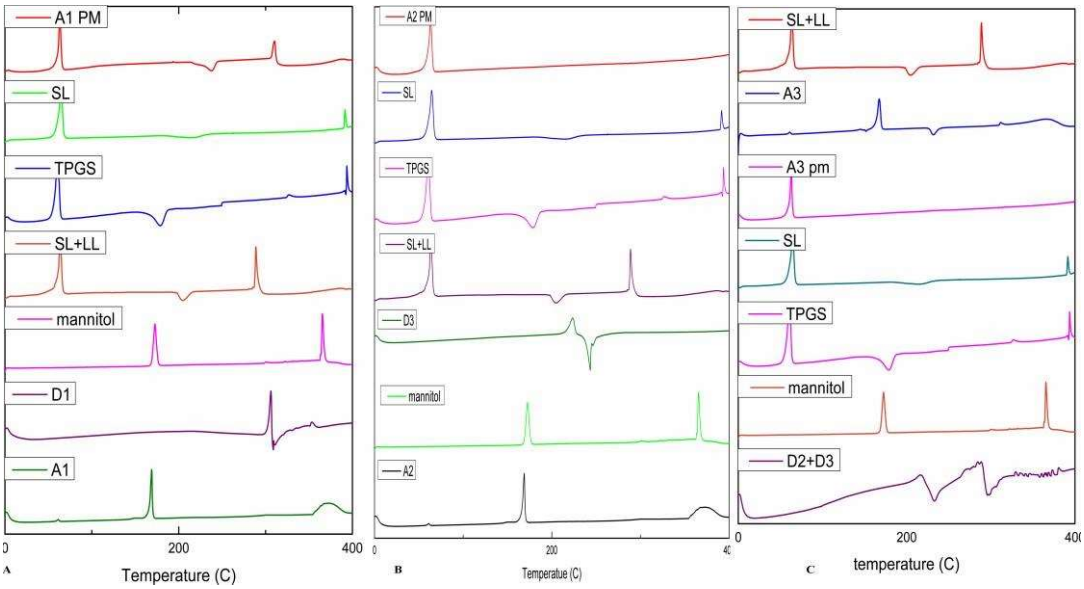

Figure 5.15: DSC thermograms of (A) Genistein (D1) and Gen loaded NLCs (A1). (B) Paclitaxel (D3) and PTX loaded NLCs (A2), (C) combination of both drugs (D2+D3) and their NLCs (A3), physical mixture (A1, A2, A3 PM) and all excipients.

Powder- X Ray Diffraction study (P-XRD):

The PXRD patterns of pure drug, lipid mix, surfactant, and the optimized formulation were examined during the study as shown in figure 6. Genistein (D2) showed numerous peaks at Θ angle of approx 7˚, 9˚, 10˚, 11˚, 15˚& 20˚ and numerous minor peaks upto 30˚ (Figure 5.16(A). PTX (D3) showed characteristic distinctive peaks at Θ angle of approx 5˚, 8˚, 15˚, 18˚& 20˚ and numerous minor peaks up to 35˚, Figure 5.16(B). In Figure 5.16(C), D2+D3 (combination of PTX+Gen) retained all the major peaks of both drugs. Also, TPGS possessed a halo containing peaks near 18 to 28˚ approximately indicating the crystalline nature of the surfactant. The optimized lyophilized formulations (A1, A2 & A3 without mannitol) also showed broad diffused halo retaining the peaks of lipid mix & surfactant at same diffraction angle. The diffraction

pattern of A1, A2 & A3 had indicated that all characteristic intense peaks of PTX & Gen had abridged in their intensity and made a diffused broad halo which confirmed the physical state of drugs that had been converted from crystalline towards amorphous state (13).

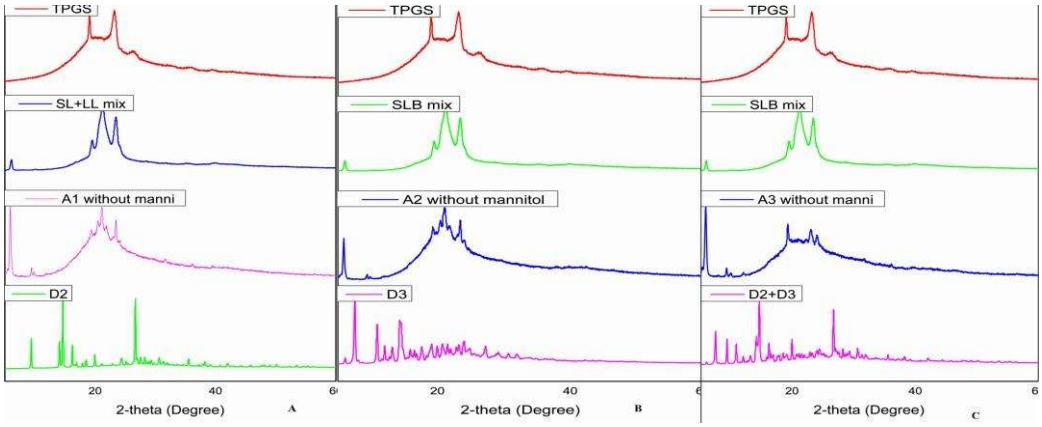

Figure 5.16: P-XRD spectra of (A) Genistein (D2) and Gen loaded NLCs (A1). (B) Paclitaxel (D3) and PTX loaded NLCs (A2), (C) combination of both drugs (D2+D3) and their NLCs (A3) and all excipients.

Particle size (PS), Polydistersity index (PDI), Zeta potential (ZP) & Entrapment efficiency (EE):

Particle size analyzer (Delsa Nano C) was used to calculate the three parameters (PS, PDI & ZP) which works on the phenomenon of Brownian motion, and light scattering whereas the value & charge of zeta potential are determined by the chemical nature of the drug, polymer, & most importantly on the nature of surfactant used. The values of PS, PDI & ZP of the optimized formulations are given in Table 5.13. The magnitude of the zeta potential charge was large enough to keep the particles apart and hence confirms the stability of the formulation (11, 56, 59, 63, 64). Also, the negative charge of the nanoparticles will delay their protein binding and thereby results in longer

circulation half-life of the nanoparticles. The PDI values of the formulations affirmed that the fabricated nanoparticles were of excellent nano range and the size was uniform throughout the formulation (65, 66). The entrapment efficiency shows that the optimized formulations can entrap sufficient amount of drug inside to release the appropriate amount of drug over an extended period of time.

Table 5.13: Particles size, PDI, zeta potential & entrapment efficiency of optimized formulations.

Formulation	PS (nm)	PDI	ZP(mV)	EE (%)
A1	118.32±4.23	0.113±0.002	-21.71±1.19	94.3±2.35
A2	122.56±6.59	0.115±0.003	-19.36±2.36	93.4±3.43
A3	127.87±1.28	0.117±0.002	-22.86±3.11	92.17±2.19 (Gen), 93.11±2.54 (PTX)

Surface morphology studies:

The prepared formulations were observed under TEM & AFM to study the size as well as surface morphology of the prepared NLCs which were found to be in the range of 130- 150 nm size throughout the image area as shown in Figure 5.17(A-C) & 5.18(A-C). The size observed under the microscope was also acquiescent with the particle size observed under particle size analyzer. The AFM image concluded the uniformity of surface of the nanoparticles.

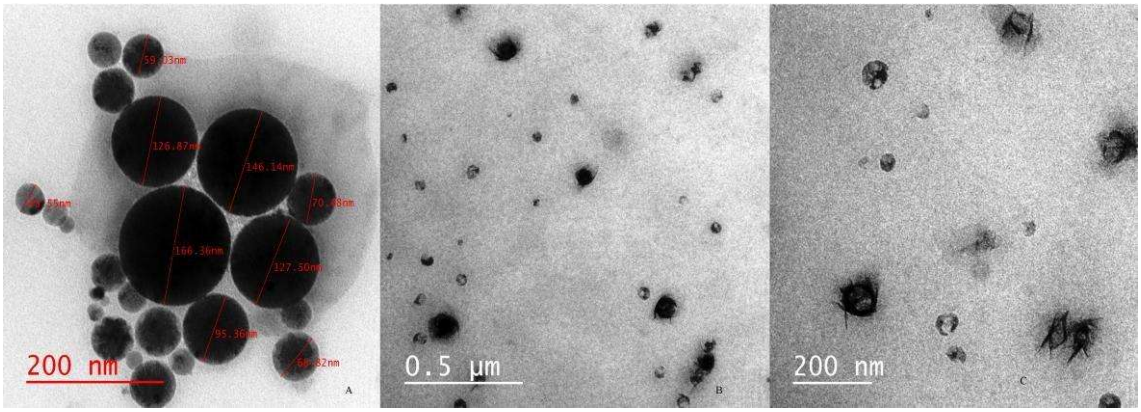

Figure 5.17 (A-C): Transmission electron microscopic images of optimized formulations (A- Gen NLCs, B- PTX NLCs & C- Gen+PTX NLCs).

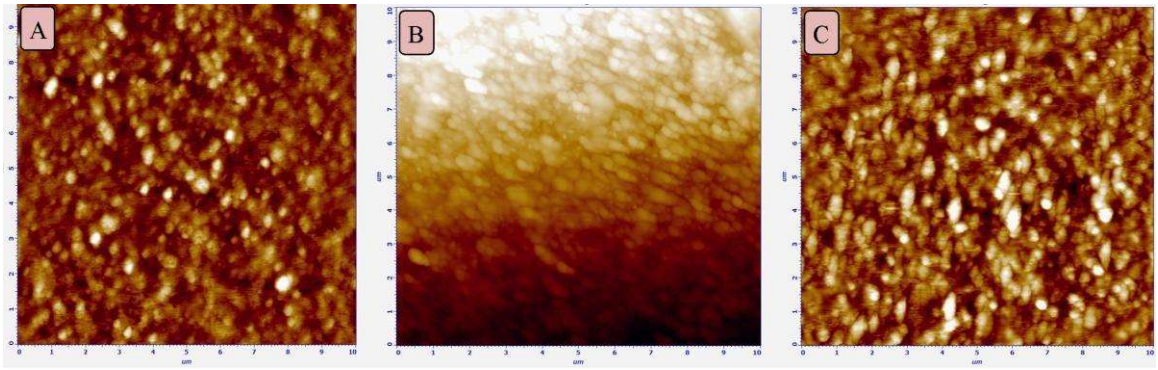

Figure 5.18 (A-C) Atomic force microscopic (AFM) images of optimized formulations (A- Gen NLCs, B- PTX NLCs & C- Gen+PTX NLCs)

Cumulative percentage drug release study:

In vitro release profiles of optimized NLCs (A1, A2 & A3) in comparison to their pure drug suspensions (Gen & PTX respectively) are shown in Figure 5.19 & 5.20. Almost complete release of the drug was observed for PTX pure drug in 24 hours(49). Approximately 87% of the PTX was released from A2 formulation & 92% of PTX from A3 formulation in 4 days. The release of PTX from the formulations did not show any

burst release which can be due to the lack of free drug present in the formulations. Further, the formulation exhibited prolonged release due to the presence of lipid matrix system which can be explained on the basis of strong affinity of the drug for the lipidic system which also provides the lipid barrier to curtail the immobilization of drug from the matrix system. Biphasic release pattern was observed for the release of drugs from the NLC system. The unentrapped drug present in the formulations was responsible for the burst release of the drug during the initial period (47) while the entrapped drug was responsible for the delayed release of the formulation. Approximately 62% of Genistein was released from A1 formulation & approximately 67% of Gen was released from A3 formulation till the end of 4^{th} day whereas the drug release from pure drug suspension was about 22% when given alone & approximately 26% in combination at the end of 24 hrs. We also analyzed the release mechanism of all formulations by substituting the release profile and time data to various kinetics models their correlation coefficient and release exponent values are mentioned in Table 5.14. From the values of R^2, it was concluded that release kinetics of nanoparticles followed Higuchi model of release kinetics and the fickian diffusion based release mechanism was followed as evidenced by release exponent value of Korsmeyer Peppas model which was found to be 0.464 for A2 and 0.457 for A1 ($n<0.5$ for fickian diffusion controlled mechanism)(59).

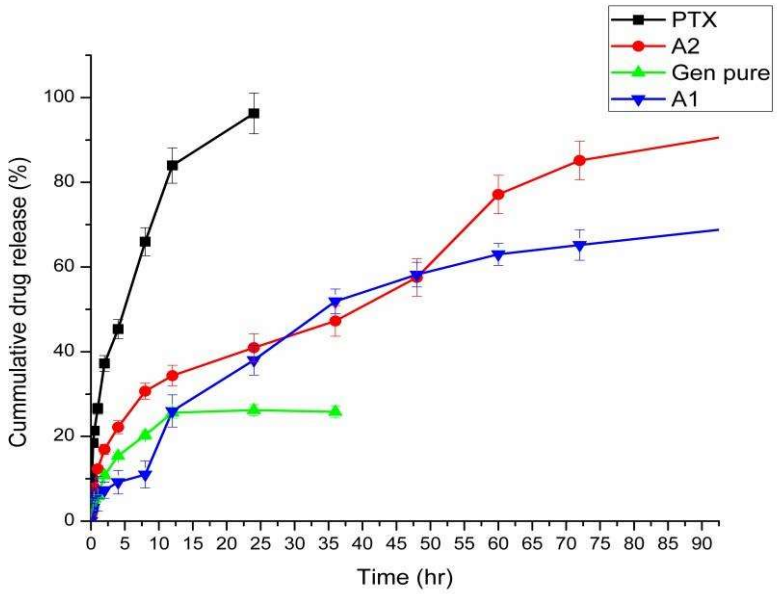

Figure 5.19: In vitro drug release profile of A1 & A2 in comparison to their pure drugs in phosphate buffer saline pH 7.4. Vertical bars represent S.D, n=3.

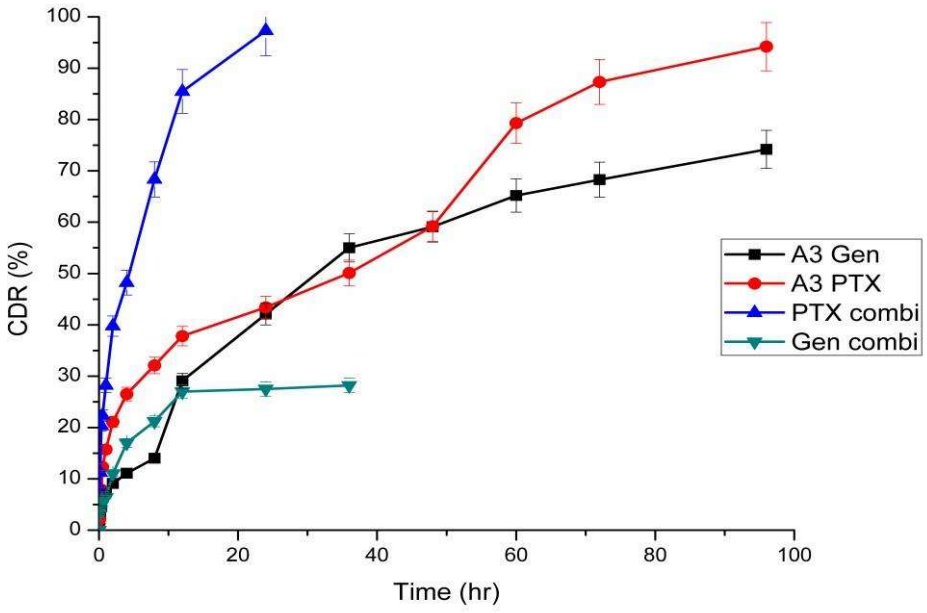

Figure 5.20: In vitro drug release profile of A3 in comparison to its pure drug combination in phosphate buffer saline pH 7.4. Vertical bars represent S.D, n=3.

Table 5.14: Correlation coefficients & release exponent values for various release kinetics models during in vitro release kineticc from optimized NLC formulation

Release Kinetics Models	A1(Gen)		A2 (PTX)	
	Correlation coefficient (R^2)	Release exponent (n)	Correlation coefficient (R^2)	Release exponent (n)
Zero Order	0.8170	-	0.825	-
First Order	0.9146	-	0.9173	-
Higuchi model	0.9840	-	0.9893	-
Korsemeyer-Peppas model	0.9821	0.457	0.9826	0.464
Release Kinetics Models	**A3 (Gen)**		**A3 (PTX)**	
	Correlation coefficient (R^2)	Release exponent (n)	Correlation coefficient (R^2)	Release exponent (n)
Zero Order	0.8192	-	0.827	-
First Order	0.9153	-	0.9178	-
Higuchi model	0.9867	-	0.9897	-
Korsemeyer-Peppas model	0.9823	0.459	0.9828	0.468

Stability Studies:

To calculate the shelf life of the formulations, stability studies were performed at different conditions of temperature and humidity. Shelf life was calculated based on percentage entrapment efficiency of the formulations which was calculated at different time periods throughout the study. Minitab® version 7 was employed to construct the shelf life graphs (Figure 5.21). Particle size, Zeta potential, PDI were also determined in comparison to fresh samples, and all these traits were found to be non-significantly different ($p>0.05$) at these conditions. The shelf life observed was about 12.8, 11.9 & 12.02 months for A1, A2 & A3 respectively at all conditions of temperature and humidity. Thus it was concluded that lipid based NLCs can be stored for sufficient period of time (55).

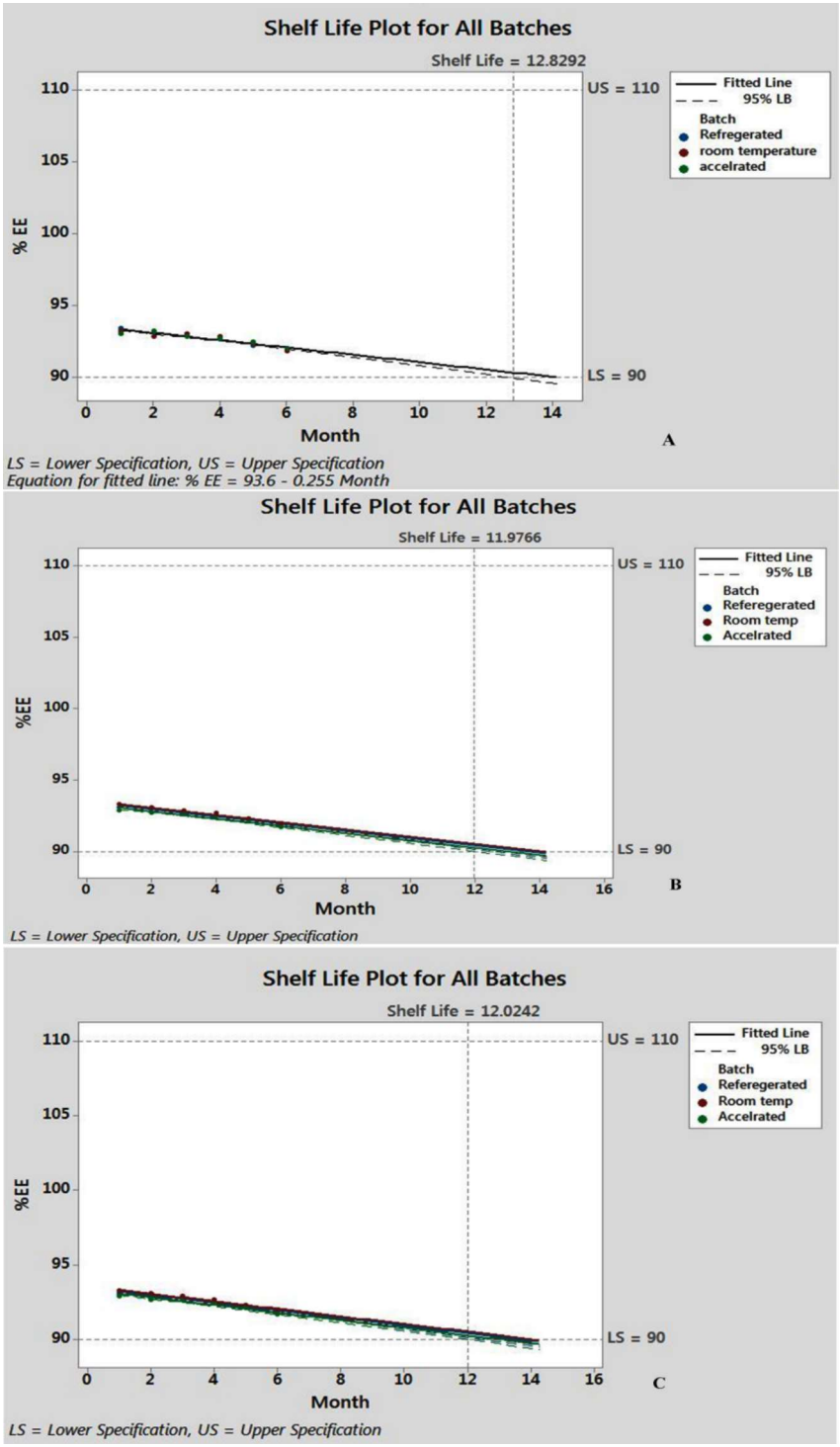

Figure 5.21: Shelf life estimation of optimized batches of NLCs (A1, A2 & A3) at various conditions.

Heamocompatibility Studies

Evaluation of haemolysis:

Haemolysis is also the most important factor for the assessment of heamocompatibility of the nanoformulations as most of the times, the formulations containing chemicals, polymers or higher concentrations of surfactants cause haemolysis of the blood cells. Therefore , haemolytic potential of formulation was determined in comparison to its placebo formulation and pure drug at 10 & 100 µg/ml. According to Brazilian standards, the limit for spontaneous haemolysis is not more than 1%. Any of the compound or formulation, intended for i.v use should not cause more than 1% of haemolysis of erythrocytes (67). In our study, all the samples caused less than 1% heamolysis throughout the study period of 8 hrs when incubated at lower concentrations i.e. 10 µg/ml but at higher concentrations (100 µg/ml), the limit of heamolysis was slightly exceeded in the last hour of the study for all the samples, which may be due to interactions of the components like capmul MCM oil and TPGS with the blood cells (46); Fig 5.22(A-C). The surfactant at a higher concentration can penetrate the cell membrane and solubilize the lipids present there. When membrane lipids are exposed to the higher concentrations of the formulation, dissolution of the membrane lipid starts which causes destruction of the erythrocytes (56).

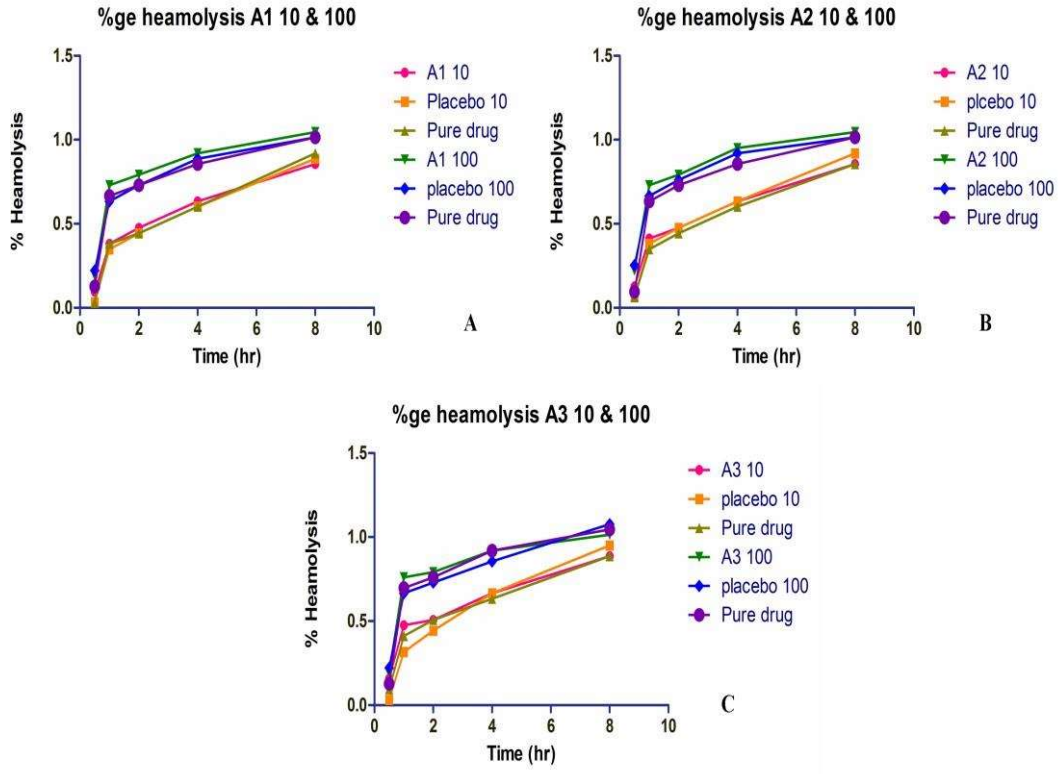

Figure 5.22: Heamolysis profiles of A1, A2 & A3 nanoparticles, placebo and their corresponding pure drugs at different concentrations.

Platelet aggregation test:

The potential of nanoparticle formulation for intravenous administration was studied by observing the platelet aggregation after addition of formulation to the citrated whole blood. Results were interpreted by visualizing the glass slides containing samples under optical light microscopy and also by counting the no. of platelets. As platelet aggregation is associated with high risk of causing myocardial infarction, transient ischemia, thromboembolism, and stroke, therefore assessment of platelet aggregation seems to be an essential part of the study. In our study, GenNLC, PTXNLC, Gen+PTXNLC, Gen, PTX, Gen+PTX, Placebo formulations and PBS at 10 & 100

µg/ml were treated with citrated whole blood, and number of platelets were counted after 30 minutes of incubation. The nonsignificant difference ($p > 0.05$) in platelet count was observed for all the samples in comparison to PBS at 10 µg/ml concentrations while at 100 µg/ml, pure drugs showed a significant decrease in number of platelets in comparison to PBS and all other groups (Figure 5.23). As the significant decrease in no. of platelets was observed for pure drugs when given alone at 100 µg/ml but not for their corresponding NLC formulations at same concentration, This observation can be explained on the basis of potential of paclitaxel in causing neutropenia and genistein‟s anticancer effect after administration while in NLC, drug was not directly exposed to blood cells and also the surfactant and lipid present also protected the blood cells from the side effects of the drug due to their antioxidant properties. In addition to the platelet count, platelet aggregation was also observed by optical light microscopy, and platelets were indicated by white arrows in the photographs in Figure 5.24. Supportively, no platelet aggregation was observed of any of the samples which substantiate the nontoxicity of NLC formulation for intravenous use (47).

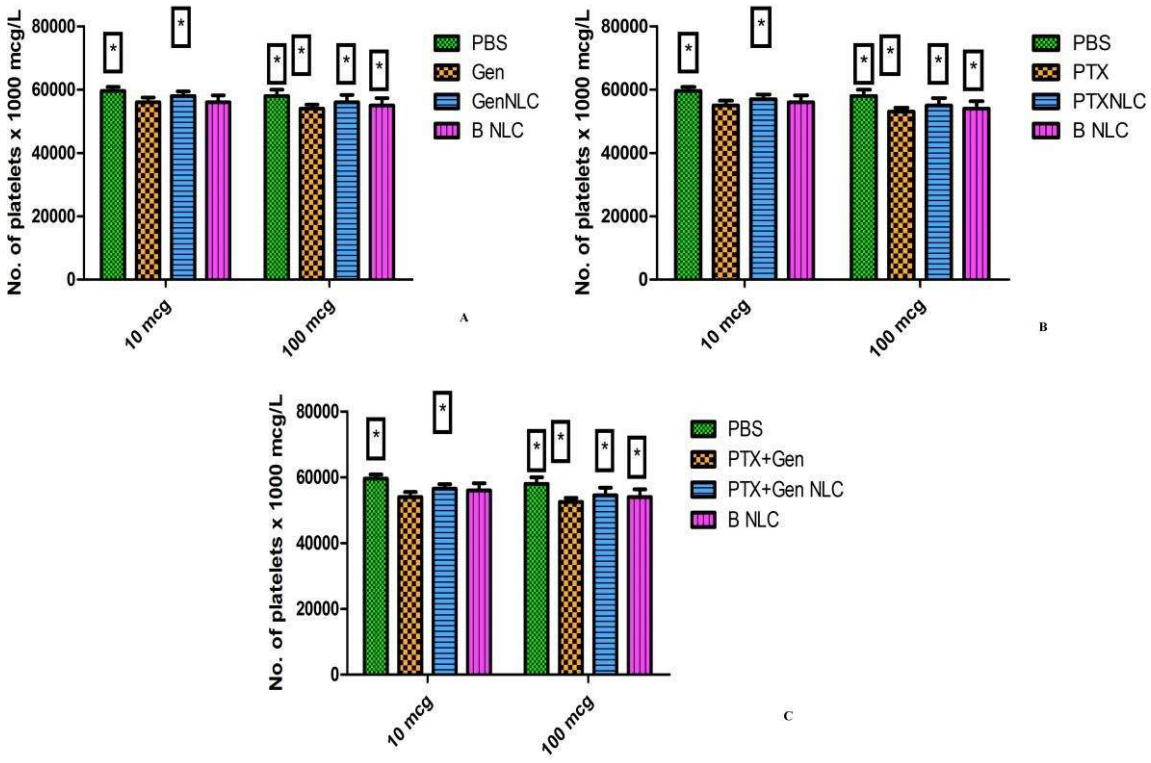

Figure 5.23: No. of platelets after addition of (A) A1, Gen (B) A2, PTX (C) A3, Gen+PTX; PBS & Placebo at 10 & 100 µg/ml. Vertical bars represent mean±SEM, n=3. *Data is non significantly different at p>0.05 from PBS (negative control).

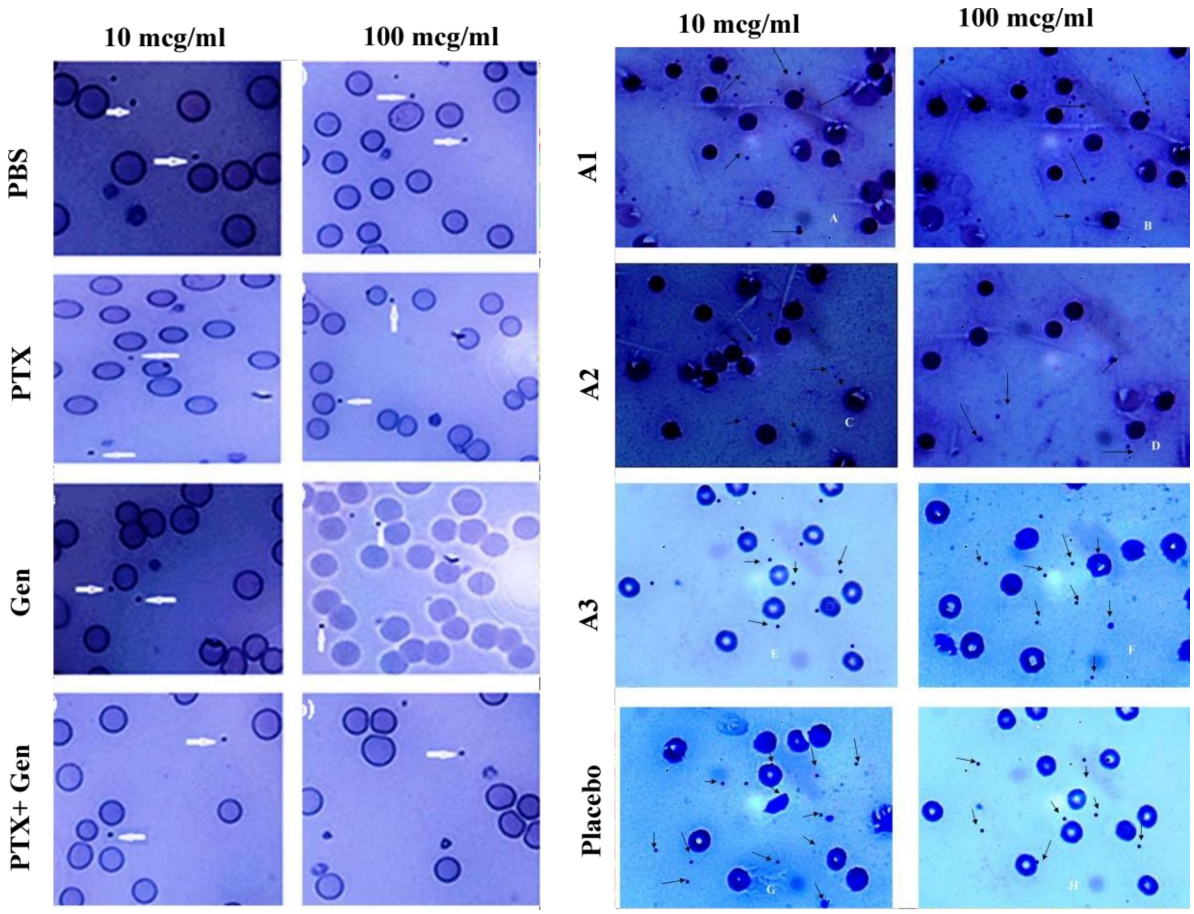

Figure 5.24: Platelet aggregation optical microscopy images of Leishman's stained whole blood samples after treatment with PBS, pure drugs (PTX, Gen & PTX+Gen) at 10 & 100 µg/ml, Placebo formulation at 10 & 100 µg/ml & optimized formulations (A1, A2 & A3) at 10 & 100 µg/ml. Images were captured at magnification of 100x.

Cytotoxicity studies:

In vitro cell line studies were performed on PA-1 cell lines. 100 µM solutions of Gen, PTX, Gen+PTX, A1, A2 & A3 were prepared in distilled water as stock solutions. From the stock, dilutions were made in the range 10 to 50 µg mL^{-1}. Cells in conc.1 $\times 10^4$ cells per well were incubated in 96 well plated for 48 h and then treated with the prepared dilutions. Placebo of the formulation was taken as positive control during the studies and normal saline as negative control. Results are shown in Figure 5.25. Among PTX and Gen, PTX was more effective in controlling the cell growth at all concentrations

($p<0.05$). PTX NLC formulation was more effective in controlling cell growth then Gen NLC at higher concentrations. At higher concentrations, the combination of drugs was equally effective to PTX in controlling the cell growth at $p>0.001$, similarly the cytotoxic potential of the combination formulation (A3) was also found to be almost equal to the PTXNLC (A2) at higher concentrations ($p>0.0001$). Cytotoxic potential was also observed for the placebo formulation to the minor extent which can be explained on the basis of cytotoxic potential of TPGS present in the formulation. (47, 68). The enhanced cytotoxic potential by TPGS will provide adjuvant therapy to treat ovarian cancer.

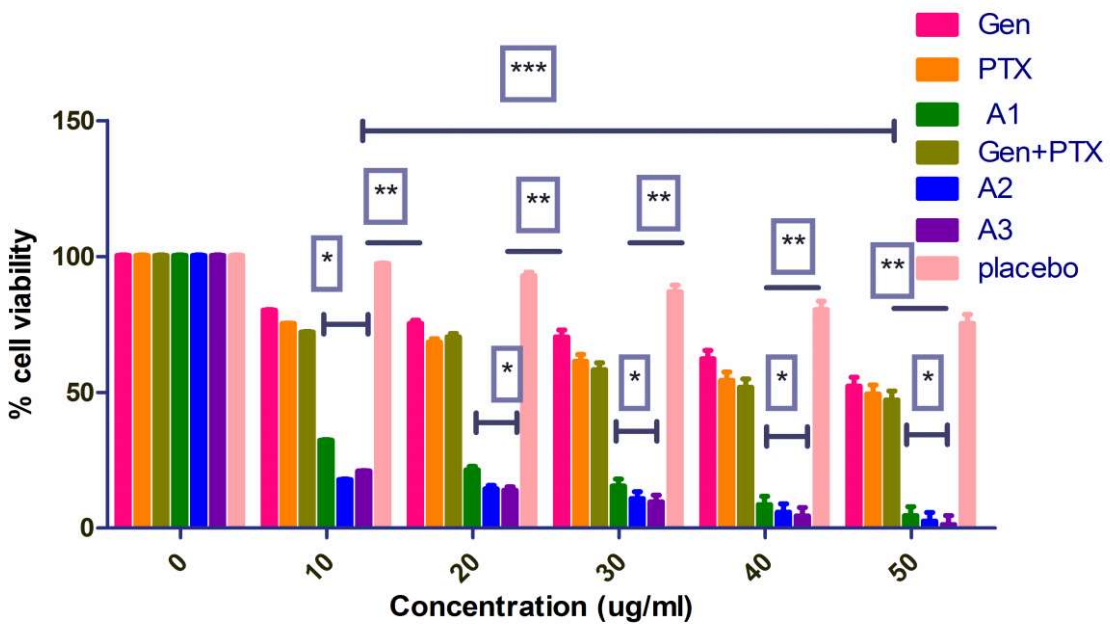

Figure 5.25: % cell viability of pure drugs (PTX, Gen & PTX+Gen), optimized formulations (A1, A2 & A3) & placebo at different concentrations. Results were analyzed by two way ANOVA followed by bonferroni posthoc test; *: when compared with pure Gen at $p< 0.05$, **: when compared with pure PTX $p< 0.001$, *: when compared with Gen+PTX $p< 0.0001$; Values are expressed as mean± SEM, n=3.**

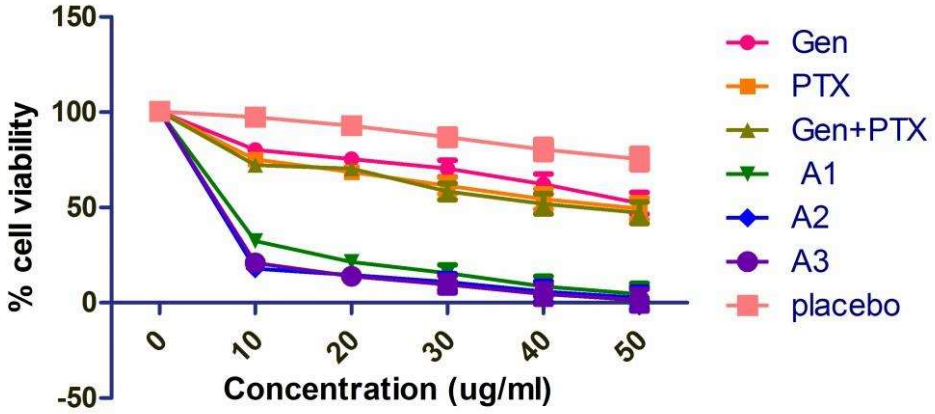

Figure 5.26: Scatter plot for the calculation of IC_{50} value.

IC_{50} values were also calculated by using curve fitting method as shown in Figure 5.26. IC50 values for Gen, PTX, Gen+PTX, A1, A2 & A3 were 61.2, 55.4, 50.8, 8.1, 5.2 & 3.3 µM respectively. IC_{50} of A1 was reduced to 7.6 fold as compared to pure Genistein. Similarly, IC50 of A2 was reduced to 10.6 folds and IC50 of A3 was reduced to 15.3 fold as compared to pure PTX and their combination respectively. Enhanced cytotoxicity of the nanoparticles over pure drug solutions can be due to the enhanced cellular uptake of the nanoparticles by reticuloendothelial system (RES). Free drug crosses the cell membrane through diffusion whereas nanoparticles were taken by cells through special internalization pathway and releases the drug in a systematic manner. Cytotoxicity of the combination (A3) was almost equivalent to the individual PTX which concludes that combination of PTX and Gen (5:1) nanoparticles can be used for the treatment of ovarian cancer in place of Pure PTX which will produce lesser side effects to the subjects.

Pharmacokinetic study:

Pharmacokinetics study was performed to evaluate the fate of the administered drug in the form of nanoparticles as its pure drug administered via intravenous route. Plasma

drug concentrations in rat plasma at different time intervals were measured up to 96 hrs. The plasma drug concentration vs. time profiles are shown in Figure 5.27& 5.28 and their corresponding pharmacokinetic parameters are shown in Table 5.15. Pharmacokinetic analysis was performed by using PK solver add in of Microsoft excel. From the Figure 5.27, it can be seen that mean plasma concentrations decreases bi exponentially in all the groups. Initially the mean plasma concentration was higher for the group treated with PTX pure (alone as well as in combination) but it was rapidly eliminated from the circulation. Encapsulation of PTX in solid liquid lipid matrix retarded the clearance of the drug thereby the formulation was able to maintain drug concentration at higher levels for prolonged periods of time. Similar behavior was observed for pure genistein (alone as well as in combination) and its formulations (A1 & A3) but the plasma drug concentration of pure Gen was lower as compared to pure PTX. Prolonged circulation of the Genistein NLC formulation was further confirmed by 2.45 fold increase in AUC when compared to its pure drug and 2.26 fold increases in AUC for PTX NLC when compared with pure PTX. Elimination half life was also improved ($p<0.05$) for both the formulations. For combination NLC (A3) formulation (Figure 5.28), AUC was enhanced by 1.5 folds for Gen and 1.7 folds for PTX when compared with the respective pure drugs in combination & $t_{1/2}$ of the A3 formulation was increased by 11.5 folds for Gen and 22.5 folds for PTX in comparison to its pure combination.

Mechanism behind these observations could be the prolonged release provided by the lipid components which decreases the body clearance. It suggests that lipid nanoparticles incorporated with combination of PTX & Gen could be a preferred tool

for the prolonged systemic circulation and longer retention of drug molecules. The release of lipid nanoparticles is usually slower since the loaded drug is needed to transfer from lipid to aqueous phase first. Thus NLCs produces higher plasma concentrations. (34, 36, 57, 69).

Table 5.15: Pharmacokinetic parameters of pure Gen, PTX, their combination Gen+PTX and their corresponding NLC formulations (A1, A2 &A3)

Groups	C_{max} (ng/ml)	AUC ({ng/ml}*hr)	$t_{1/2}$ (hr)
Pure PTX	5400.03	31666.83191	7.07
Pure Gen	4300.02	21111.22128	6.89
Pure Gen in Gen+PTX	3823.098	24314.76	8.5
Pure PTX in Gen+PTX	5600.23	22810.87	4.8
Gen in A1	2955.453	51836.18619	55.67
PTX in A2	3654.66	71695.96737	38.41
Gen in A3	2600	60978.77	92.01
PTX in A3	3421	72557.55	122.09

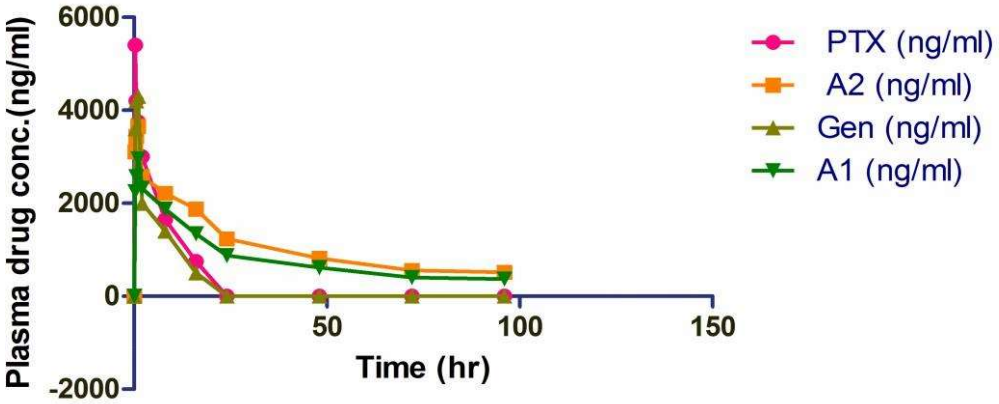

Figure 5.27: Comparative plasma drug concentration vs. time profile of Gen, PTX, A1, & A2 after intravenous administration. Dose administered was 10 mg/kg. Each data point represents mean ± SEM, at $p<0.05$.

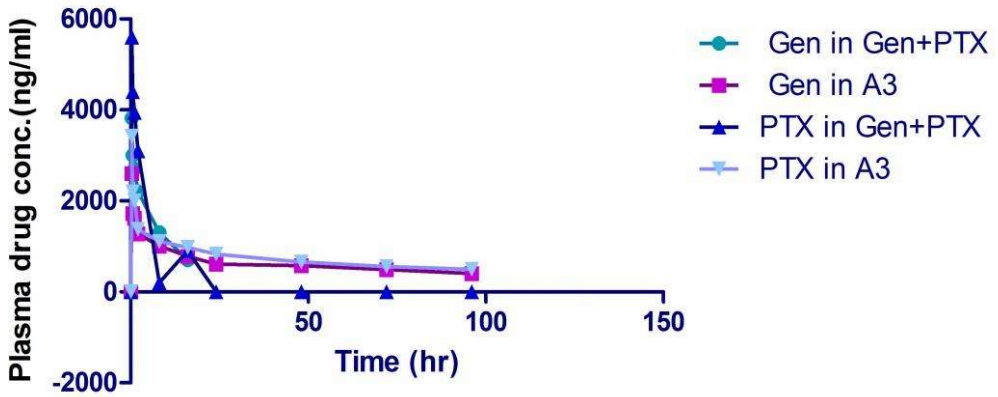

Figure 5.28: Comparative plasma drug concentration vs. time profile of Gen & PTX in pure drug combination, Gen & PTX in combination formulation after intravenous administration. Dose administered was 10 mg/kg. Each data point represents mean ± SEM, at $p<0.05$.

Table 5.16: Plasma drug concentration (PDC in ng/ml) and time (hr) data of pure PTX, Gen and their corresponding formulations (A1 & A2)

Time	PDC (PTX) (ng/ml)	PDC A2 (ng/ml)	PDC (Gen) (ng/ml)	PDC (A1) (ng/ml)
0.00	0.00	0.00	0.00	0.00
0.25	5400.03	3112.66	3600.02	2250.45
0.50	4200.07	3445.22	4200.00	2567.33
1.00	3750.00	3654.33	4300.00	2955.33
2.00	3000.15	2578.32	2000.10	2322.74
8.00	1651.09	2219.13	1400.00	1877.22
16.00	750.84	1876.14	500.56	1344.22
24.00	0.00	1234.25	0.00	874.24
48.00	0.00	814.40	0.00	616.51
72.00	0.00	556.81	0.00	402.57
96.00	0.00	514.79	0.00	372.19

Table 5.17: Plasma drug concentration (PDC in ng/ml) and time(hr) data of pure PTX , Gen in pure drug combination and in combination formulation (A3)

Time	PDC Gen PTX+Gen (ng/ml)	PDC Gen A3 (ng/ml)	PDCPTX PTX+Gen (ng/ml)	PDC PTX A3 (ng/ml)
0.00	0.00	0.00	0.00	0.00
0.25	3823.65	2600.77	5600.03	3421.00
0.50	3000.98	1723.55	4400.00	2198.00
1.00	2700.43	1622.35	3950.00	2000.00
2.00	2200.23	1276.21	3100.00	1378.00
8.00	1300.65	1011.12	200.00	1111.00
16.00	700.24	782.76	900.00	979.00
24.00	0.00	612.56	0.00	832.00
48.00	0.00	576.88	0.00	654.00
72.00	0.00	489.12	0.00	554.00
96.00	0.00	402.11	0.00	498.00

In vivo biochemical estimations:

In vivo biochemical estimations were made in order to evaluate the blood serum parameters in respect of liver toxicity (SGOT, SGPT, ALP & Total Billirubin) and Neutropenia (Absolute Neutrophil Count (ANC) after the administration of prepared formulations by i.v route at a dose of 10 mg/kg. Pure saline (0.9% NaCl) was kept as control and pure drugs were also evaluated for their comparisons with the respective formulations. From the results as shown in Figure 5.29, it was inferred that pure PTX increased the level of ALP, AST and TBIL and decreased level of ALT which proved

liver damage. Decrease in neutrophil count was also observed by both pure PTX & pure drug combination. The toxic effect of PTX on neutrophils was less pronounced with A2 and least with A3. Significant difference ($p < 0.0001$) between neutrophil count was observed when A2 (PTX NLC) was compared with control. Non significant difference ($p > 0.0001$) was observed when A3 (combination NLC) was compared with control. Entrapment of drug (PTX) in lipid matrix decreased the toxic effects caused by pure drug but the masking of toxicity was not upto the mark. So to reduce the toxicity of PTX, we entrapped PTX along with Gen which is a phytoconstituent possessing antioxidant property along with anticancerous properties for ovarian cancer. Thus, the toxicity of PTX was efficiently masked when Gen was incorporated along with PTX in a ratio of 1:5 (Gen:PTX). So, the ratiometric combination of phytoestrogen along with chemotherapeutic semi synthetic drug had been proven to be safe and equally effective medication for the treatment of ovarian cancer.

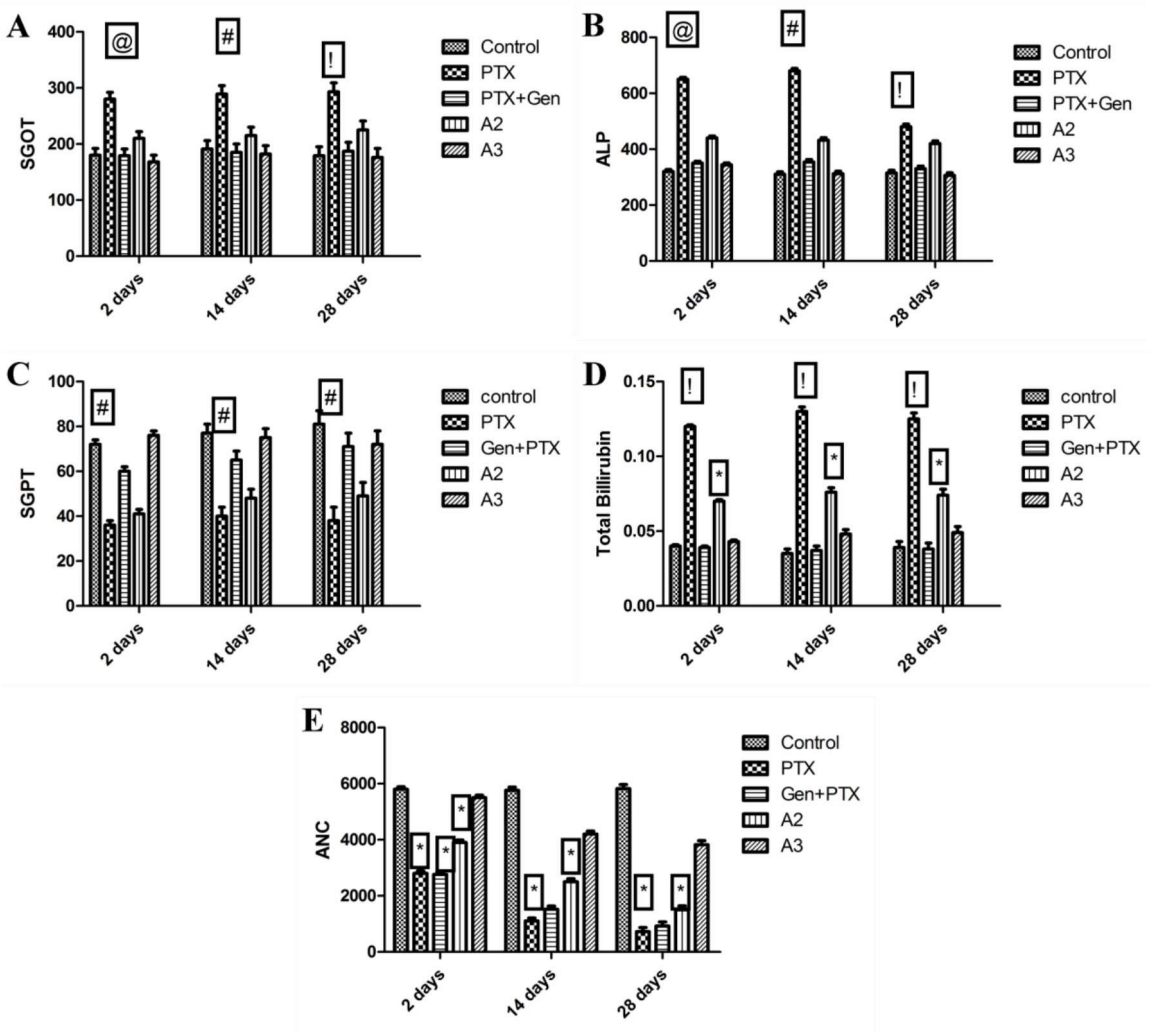

Figure 5.29. Blood serum levels of (A) Aspartate aminotransferase (AST or SGOT) (B) alkaline phosphatase (ALP), (C) alanine transaminase (ALT or SGPT) (D) Total billirubin and (E) absolute neutrophil count (ANC) after the administration of A2 & A3 which were compared with their respective pure drugs at a dose of 10mg/kg. 0.9% saline act as control. Each data point represents Mean ± SEM, @ at p< 0.0001, # at p< 0.001, ! at p<0.05 and * at p< 0.0001 as compared to control.

5.2.16 In vivo anticancer study:

In vivo anticancer study was performed in Balb/c mice of age about 8-10 weeks by injecting ID-8 murine epithelial ovarian cell line. A significant decrease in % tumour growth tumour volume & relative tumour volume was observed for A3 formulation in comparison to non treated & pure drug combination group, however, the % tumour growth for the group treated with standard (doxorubicin, i.v) was almost same to the group treated with formulation at different time intervals (Figure 5.30-5.32). All the groups showed 100% survival during the study and their body weight at the end of the study was also found in the desired range in comparison with initial weight. Thus the combination of synthetic drug along with phytoconstituent provide the synergistic effect for the treatment of ovarian cancer and offered least toxicity to the subjects.

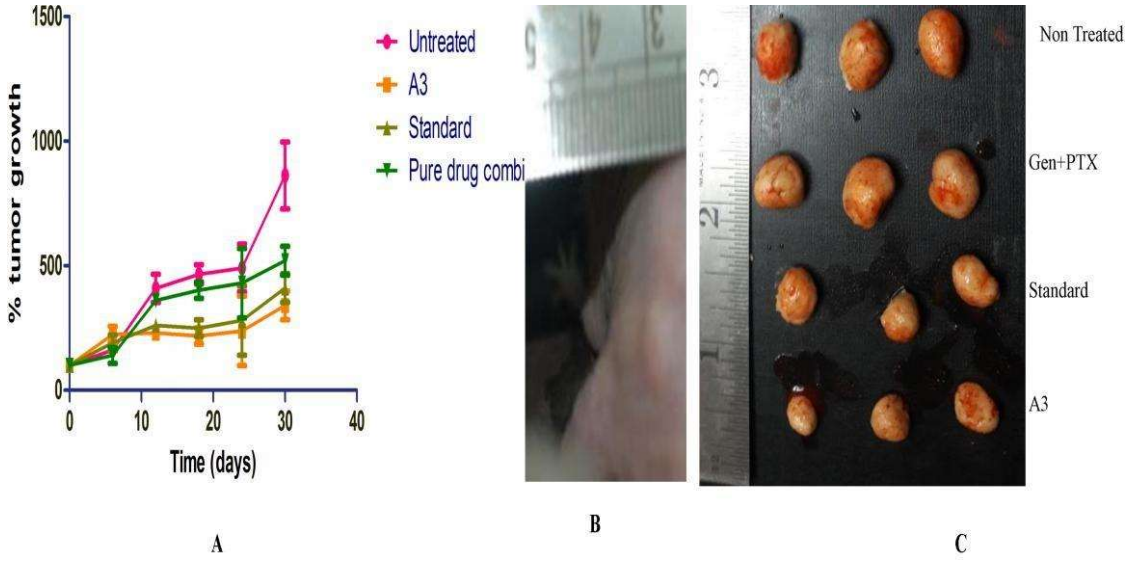

Figure 5.30: (A) Graphical representation of % tumor growth vs. time (days) with treatments administered i.v. on the days mention on the graph. Error bars represent SEM, n=3, p value <0.001. (B) Representative image of tumor (c) Images of whole excised tumors for different test groups.

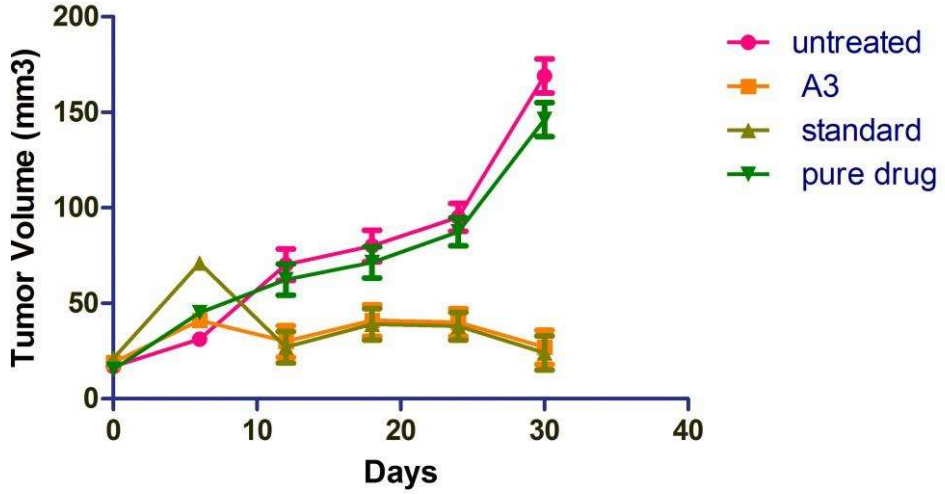

Figure 5.31: Tumor volume of combination formulation; A3 in comparison to its pure drug combination. Results were analyzed by two way ANOVA followed by bonferroni posthoc test ; (@p< 0.001) & (# p<0.0001).

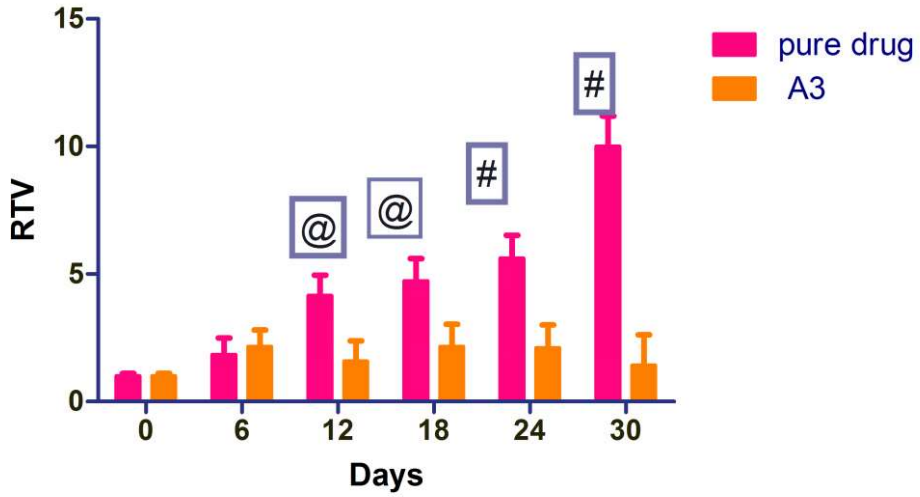

Figure 5.32: Relative tumor growth rate of combination formulation; A3 in comparison to its pure drug combination. Results were analyzed by two way ANOVA followed by bonferroni posthoc test ; (@p< 0.001) & (# p<0.0001).

Result & Discussion of polymeric nanoparticles:

Experimental design:

A 3 factors, 3 level (3^3) response surface based Box Behnken design (BBD) was utilized to study the impact of independent variables {i.e. polymer concentration (X1), surfactant concentration (X2) and amount of organic solvent (X3)} on dependent variables {i.e. particle size (Y1), poly dispersity index (Y2) & entrapment efficiency (Y3)} which was comprised of 17 no. of experimental runs (Table 5.18 & 5.19). The results were analyzed by the principles of analysis of variance (ANOVA) using Design expert® software at 95% confidence interval. Results for the each dependent variable were generated in the form of quadratic equations from which the best fitting of the model was resolved by their corresponding F& P values. Lack of fit, Regression coefficient & coefficient of variation were also calculated who helped to have an idea about the reliability and precision of the chosen model. The dependency of the independent variable on the dependent variable was analyzed by the coefficient values of corresponding factor for each response and the positive sign of the coefficient indicated the direct and negative sign indicated the indirect relationship of that factor for that particular response. Further, contour plots and 3D surface plots were constructed to demarcate the interactive effects of 2 independent variables on dependent variable as depicted in Figure 5.33-5.35. Results of the quadratic models analysis were depicted in the form of lack of fit value as well as p-value (11, 55, 59).

Table 5.18: Summary of 3 factor 3 level Box Behnken design

Study Type	Response Surface	**Runs**	17
Initial Design	Box-Behnken	**Blocks**	No Blocks
Design Model	Quadratic		

Factor	Name	Units	Type	Low (-1)	Medium (0)	High (+1)
X1	Polymer conc.	%	Numeric	0.2	0.35	0.5
X2	Organic solvent	ml	Numeric	5	7.5	10
X3	Surfactant conc.	%	Numeric	0.75	1.0	1.5

Response	Name	Units	Obs	Analysis	Minimum	Maximum	Constraint
Y1	PS	nm	17	Polynomial	112.700	391.000	Minimize
Y2	PDI		17	Polynomial	0.113	0.213	Minimize
Y3	EE	%	17	Polynomial	87.33	96.54	Maximize

Table 5.19: Statistical ANOVA based results of quadratic model

Response	Quadratic model						
	F- Value	**P- Value***	**R-Square**	**R-Sq (adj)**	**CV%**	**Lack of fit**	**Remark**
P.Size(nm)	47.39	<0.0001	0.983	0.963	7.07	0.099	Significant
PDI	15.91	<0.0007	0.953	0.893	4.39	0.91	Significant
EE (%)	15.47	<0.0008	0.9521	0.890	0.97	0.30	Significant

R-Sq (adj)= R Square adjusted; CV= Coefficient of variation

*p-value<0.05 is considered as statistically significant.

Table 5.20: Box Behnken experimental design representing experimental runs with different combinations of input factors

No. of runs	Polymer (PLGA 75:25) conc.%	Amount of organic solvent (ml)	Surfactant conc. (%)	Particle size (nm)	PDI	% Entrapment efficiency
1.	0.50	5.00	1.13	233.266	0.170016	91.1711
2.	0.35	5.00	1.50	243.285	0.139656	94.7232
3.	0.50	10.00	1.13	391.037	0.148764	90.4728
4.	0.20	7.50	0.75	154.128	0.19228	89.3596
5.	0.35	7.50	1.13	161.718	0.150788	94.7232
6.	0.35	7.50	1.13	150.08	0.169004	94.3184
7.	0.35	7.50	1.13	169.409	0.170016	93.9136
8.	0.35	10.00	0.75	275.669	0.191268	90.3716
9.	0.35	7.50	1.13	176.189	0.169004	95.9376
10.	0.35	7.50	1.13	165.26	0.154836	95.2292

11.	0.50	7.50	0.75	301.677	0.21252	87.3356
12.	0.35	5.00	0.75	222.944	0.169004	92.9016
13.	0.50	7.50	1.50	324.245	0.186208	90.4728
14.	0.20	7.50	1.50	139.858	0.16698	93.4076
15.	0.35	10.00	1.50	252.393	0.171028	96.4436
16.	0.20	5.00	1.13	127.107	0.113344	96.5448
17.	0.20	10.00	1.13	112.737	0.171028	94.7232

Table 5.21: Quadratic equation generated by Box Behnken Design

*Y	Particle size (Y1)	Polydispersity index (Y2)	Entrapment efficiency(Y3)
X_0	+164.53	+0.16	94.82
A	89.55	+9.235E-003	-1.82
B	+25.65	+0.011	-0.42
C	+0.67	-0.013	+1.88
A*B	+43.04	-0.020	+0.28
A*C	+9.21	-2.5E-004	-0.23
B*C	-10.90	+2.27E-003	+1.06
A^2	+16.46	+4.908E-003	-2.53
B^2	+35.05	-0.017	+0.93
C^2	+48.99	+0.022	-2.15

*Y= response; X_0 = intercept; A-C= Factors

Influence of variables on particle size:

The value of particle size varied from 112.7 to 391.0 nm throughout the all 17 experiments due to variations in factor combinations. The formulations were prepared by varying the drug for each experimental run randomly but all the other parameters were kept same as that stated by experimental design. The F value of our selected model was 47.35 which compiles with the standards to accept the model and non-significant lack of fit (0.0991) had also confirmed the acceptability of the model. The p value of <0.0001 suggested the best fitting of the data. The value of coefficient of variation gave

an idea about the precision and reliability of the selected model; here the low value of the same suggested that the model was much reliable and precise too. The value of R-square was in reasonable agreement with the adjusted R squared value (Table 5.19), therefore it was concluded that the chosen model can be used to navigate the design space. From the plots as well as numerical data (Table- 5.21 & Figure 5.33, it was discovered that all the 3 factors were affecting the particle size positively i.e. value of particle size will increase with increase in any of the factors. Here, the polymer (PLGA) concentration appeared to be the strongest influencing parameter for the particle size and the concentration of surfactant (poloxamer 188) appeared to affect most weakly to the same. The positive relationship of polymer concentration can be explained on the basis of increased viscosity of the contents and thereby reduction in shearing efficiency of the stirrer which will ultimately cause the particle size of the formulation to get increased (11, 55, 59, 70). The increased amount of organic solvent (Acetone) will also results in increase in particle size of the formulation, which can be explained based on the fact that acetone is a slowly evaporating solvent and it has to be kept overnight under stirring to remove it completely from the formulation. More the amount of solvent present in the formulation, more the time it will need to get evaporated and larger will be the particle size of the formulation due to coalescence of the particles. Also, it can be seen from the quadratic equation coefficient values (Table 5.21) that alone, the amount of organic solvent is less impacting the particle size but its interaction with the polymer concentration made large impact over the same response. The increase in particle size due to the interaction of both parameters can be explained with the fact that more amount of organic solvent would be needed to dissolve the extra amount of polymer present and which will ultimately lead to increased particle size due to increase in

viscosity of the organic phase as well as due to much time needed to evaporate the organic phase from the formulation. The surfactants are needed in an optimum amount for any formulation. Increase in concentration of surfactant above the optimum amount will leads to increase in particle size because the poloxamer can also be used as polymer at higher concentrations which can leads to increase in particle size due to increased viscosity of the phase (71, 72).

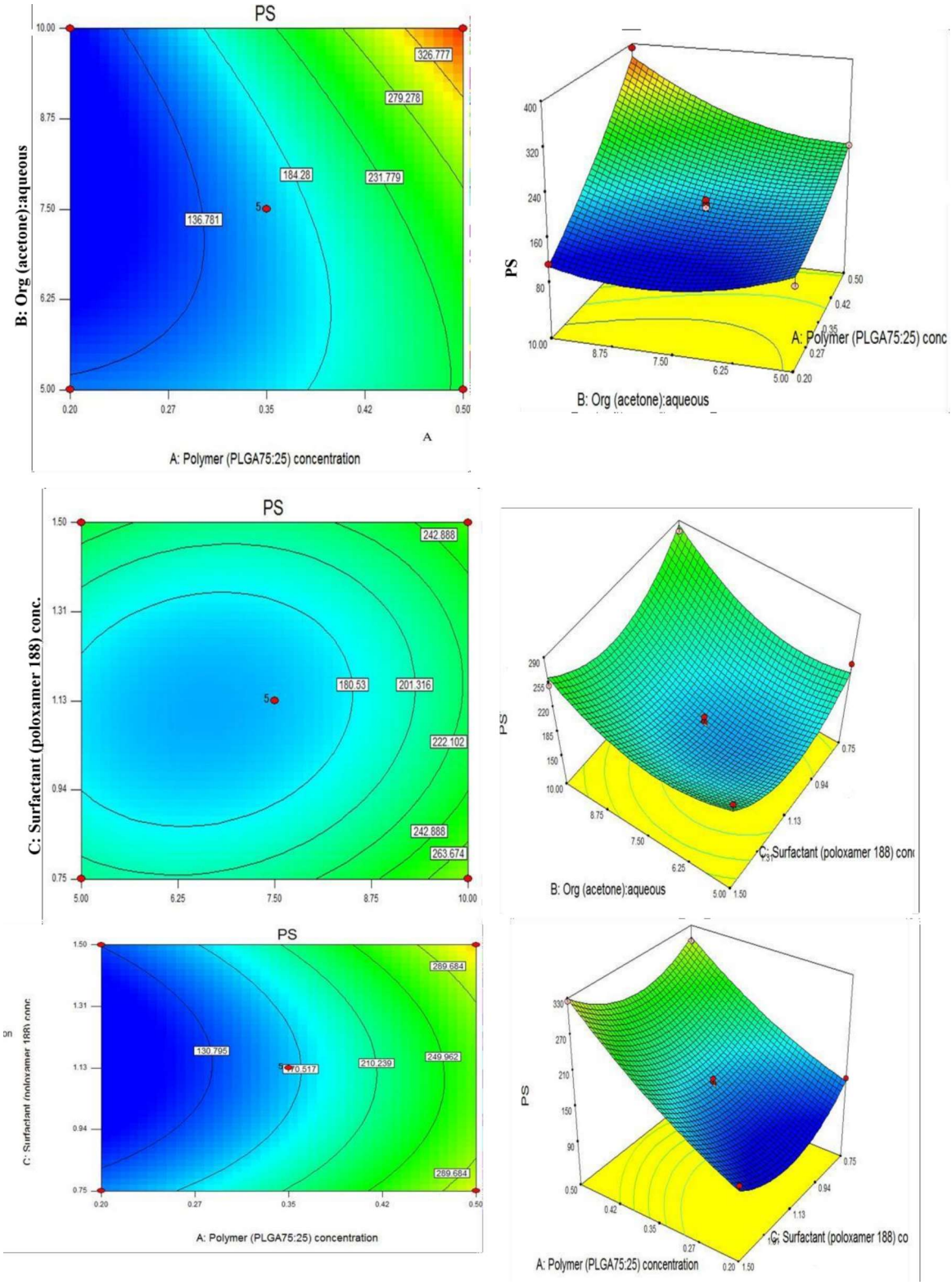

Figure 5.33: Graphical representation of effect of independent variables (Polymer concentration (X1), amount of organic solvent (X2) & Surfactant concentration (X3)) on dependant variable (particles size (Y1).

Influence of variables on polydispersity index (PDI):

The PDI varied from 0.113- 0.213 for different combinations of factors presented in the form of experimental runs. The quadratic equation generated by multiple linear regressions is shown in Table 5.21. The model was having F value of 15.91 at p value of <0.0007, which made it suitable and significant model for the given response. Also, the non-significant lack of fit (0.9172) had made it more reliable for dealing the PDI of the formulation. The precision and reliability were also reflected by the low value of coefficient of variation (4.34). A good correlation between dependent and independent factors was justified by their sufficiently high R-square value (0.9534). Values of "Prob > F" less than 0.0500 indicate model terms were significant. In this case, B, C, AB, B^2 and C^2 were significant model terms (Table 5.21). The influence of various parameters on PDI was evaluated by relating Figure 5.34 & Table 5.21, where it was analyzed that amount of organic solvent affects the response positively and the surfactant concentration has negative impact on the value of PDI. Increase in polymer concentration will increase the value of PDI owing to its direct impact on the thickness of organic phase. The Higher viscosity of the polymer matrix will suppress their segregation or will promote the aggregation of the nanoparticles by suppression of their negative charge which would result in the irregular distribution of the particles and hence higher will be the PDI(11, 59, 61). Nonetheless, significant decrease in PDI was observed with increase in surfactant concentration (X3) which can be attributed to the marked reduction in interfacial tension between aqueous and organic phase which will provide homogeneity to the particles and result in decreased PDI(11, 51, 53, 59, 62).

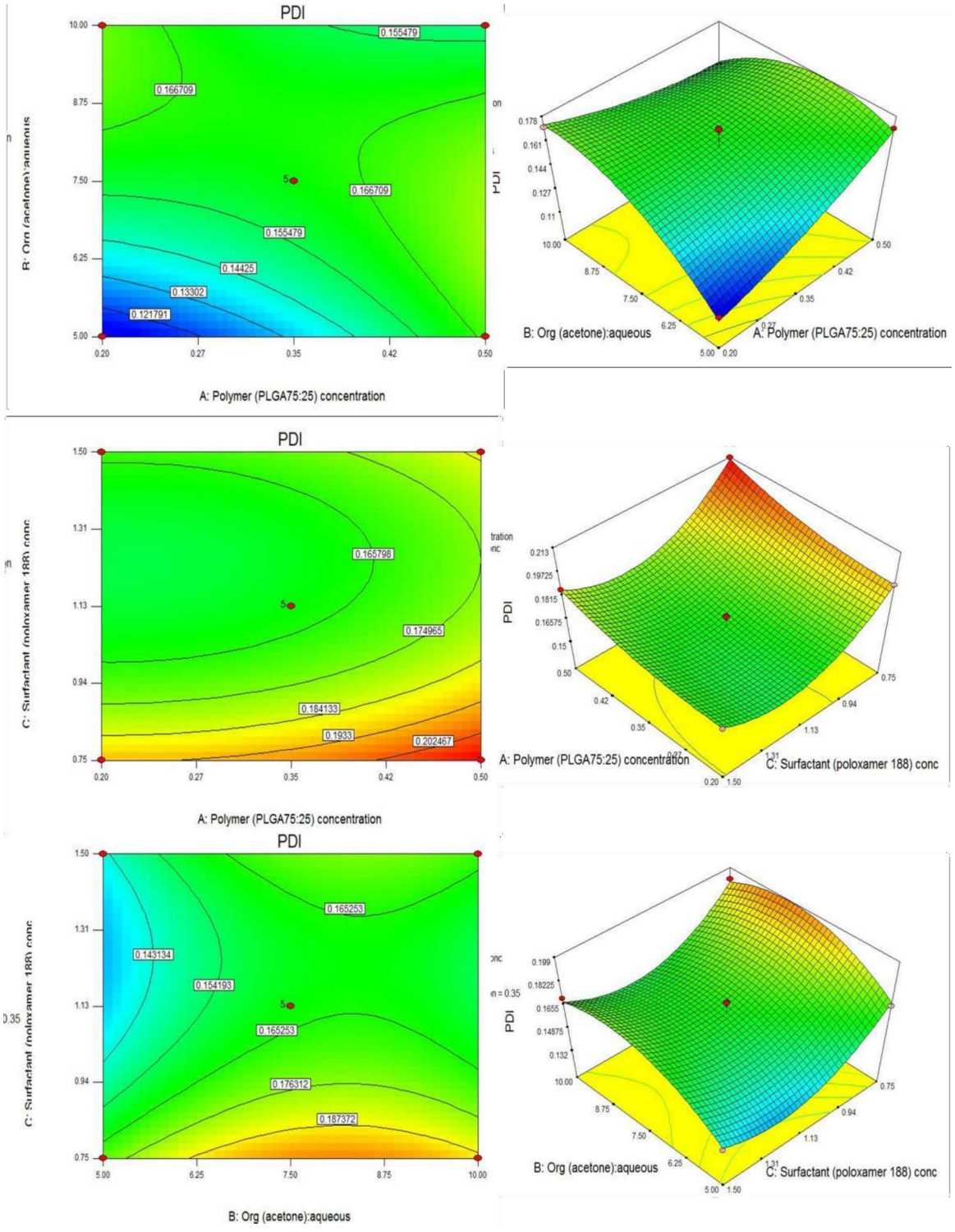

Figure 5.34: Graphical representation of effect of independent variables (Polymer concentration (X1), amount of organic solvent (X2) & Surfactant concentration (X3)) on dependant variable (polydispersity index (Y2)

Influence of variables on entrapment efficiency (EE):

To calculate the effect of variables on EE, 10 mg of both drugs and their combination was added to the formulation on randomized basis. The entrapment efficiency varied from 87.33 to 96.65% for different formulation combinations of different drugs. The F value of 15.47 at P value of <0.0008 implies that the chosen model was significant for that particular response which was also proved by the low value of lack of fit (0.307), Table 5.19. The low value of coefficient of variation (0.97) suggested that the chosen model was precise as well as reliable in analyzing the results. The good agreement of the R-square value (0.9521) with the adjusted R squared value (0.8906) suggested that this model was the right choice which can be used to navigate the design space. The quadratic equation generated because of ANOVA is shown in Table 5.21. From the equation (Table 5.21 & Figure 5.35), it was discovered that A, C, BC, AC, A^2 & C^2 were the model significant terms. The polymer concentration as well as amount of organic solvent had the negative impact on the entrapment efficiency of the nanoparticles whereas the concentration of surfactant posses the positive impact on the EE. It can be visualized from the 3 D plots of the entrapment efficiency that the polymer concentration had its mixed effect on the same means the EE of the nanoparticles will increase with increase in polymer concentration up to certain extent then after will start decreasing on further increase in polymer concentration. This behavior can be explained on the two bases: Firstly, as we go on increasing the polymer concentration, more amount of substrate will be available for the drug molecules to get dissolve and more will be the entrapment efficiency of the nanoparticles but after achieving the optimum concentration, if we further start increasing the polymer concentration, it will start thickening of the organic phase which will ultimately hinders the drug to get inside the

polymer and thus decrease the entrapment efficiency. Secondly, the relation of EE with the polymer concentration can be explained based on combined impact of polymer concentration as well as organic solvent amount. The increased polymer concentration will increase the entrapment efficiency up to certain period of time at sufficient amount of organic solvent but on further increase in polymer concentration, the increased amount of organic solvent needed to dissolve the same amount of polymer which will start leaching of the drug molecules out of the nanoparticles and thus reduces the entrapment of the drug inside the nanoparticles (60). Similarly, sufficiently high surfactant concentration is also needed to form a particle of uniform size with good entrapment efficiency as at lower surfactant concentrations, sufficient amount of drug will not be able to dissolve in the lipid medium which will further lead to decrease in entrapment efficiency (61).

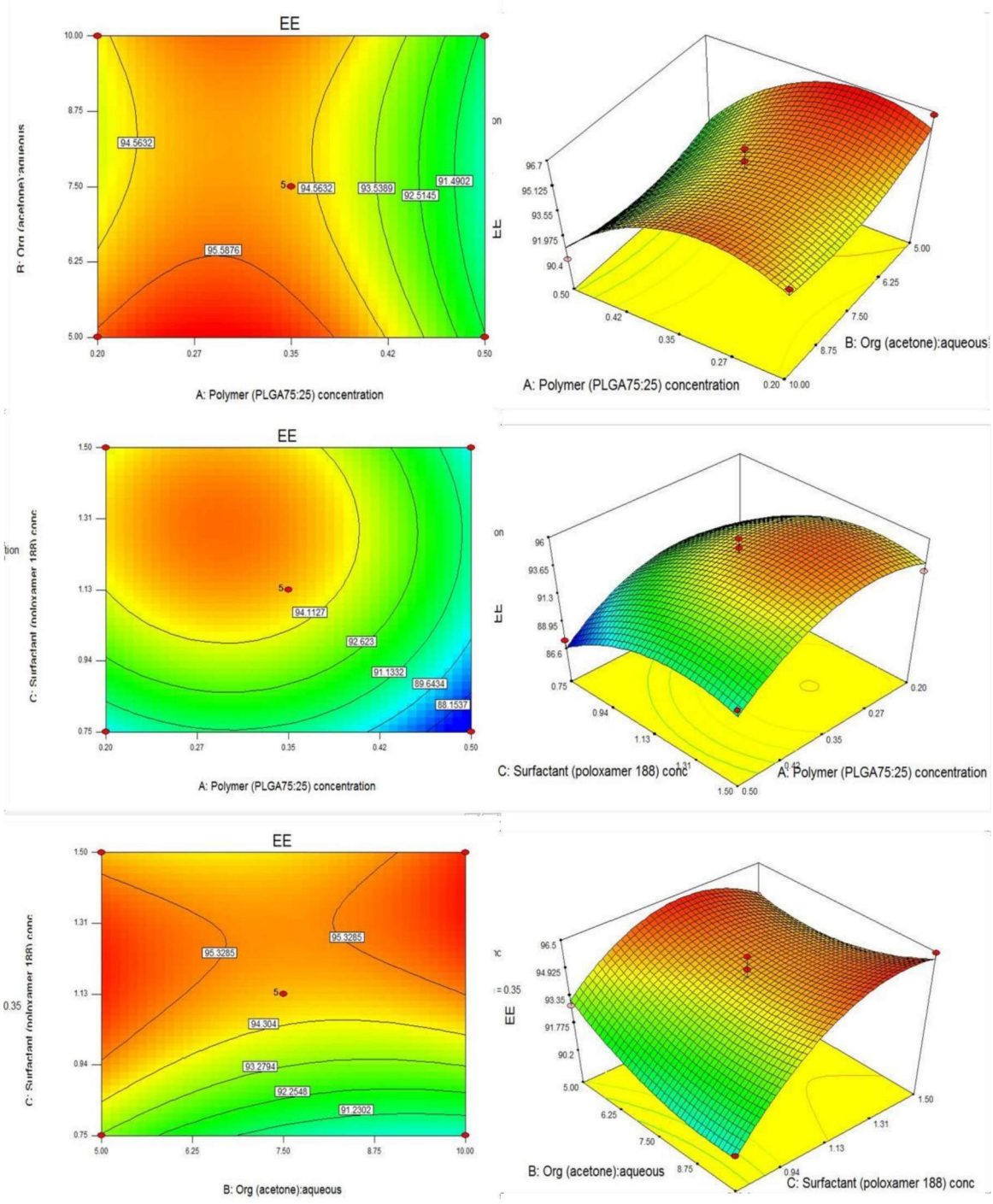

Figure 5.35: Graphical representation of effect of independent variables (Polymer concentration (X1), amount of organic solvent (X2) & Surfactant concentration (X3)) on dependant variable entrapment efficiency (Y3).

Optimization of Polymeric nanoparticles:

Numerical optimization technique based on desirability function was utilized to optimize the final formulation as it seems to be very difficult to optimize the formulations manually based on all results. By using the desirability approach, we fixed constrains for each response and the desired formulation will result in minimum particle size and PDI but maximum % EE (Table 5.22). Accordingly, the optimized formulation was formulated for confirming the validity of the software. Percentage biasness was calculated between experimental values and predicted values as shown in Table 5.22. A good agreement between the predicted and experimental values confirmed the reliability of the response surface design for optimization of PLGA nanoparticles.

Table 5.22: Desirability approach based numerical optimization of various factors

Independent Variables	Predicted Levels
Polymer conc (X1)	0.23% w/v
Amt of org solvent (X2)	5.0 ml
Surfactant conc. (X3)	1.18% w/v

Responses	Predicted value	Experimental value	% bias[a]
Particle Size	147.502 nm	142.91± 7.83 nm	3.4%
Entrapment Efficiency	96.38%	94.34±2.34%	2.11%
Polydispersity Index	0.113	0.114±0.003	-0.88%
Overall Desirability		0.948	

All results were expressed as mean ±SD, n=3. [a]Bias was calculated as {(predicted value- experimental value) / predicted value} x 100.

Fourier Transformed Infrared studies (FTIR):

The FTIR technique was employed to study the drug excipient compatibility as well as for the identification of the drugs. The FTIR spectra of PTX, nanoparticles containing

PTX (B2), Gen, Gen nanoparticles (B1), combination of PTX+Gen, nanoparticles containing combination of both drugs,1:1 physical mixture and all the excipients are shown in Figure 5.36 (A), (B) & (C) respectively. In Figure 5.36 (A), the spectra of D2 (Gen) possesses major peaks near 1500, 1700, 3000, 3050 and 3400 cm^{-1} which corresponds to amide –NH bending, Amine C=O stretch, aromatic –CH stretch, -OH stretch and secondary –NH stretch respectively. In Figure 5.36 (B), PTX (D3) exhibited peaks near 1100cm^{-1} & 1350 cm^{-1} which correspond to C-O stretch and another peak near 1350 cm^{-} and C=C stretch respectively. Two more peaks near 1680 and 1750 cm^{-1} corresponding to C=O stretch of amide and ester respectively. Further peaks near 2970 cm^{-1} , 3100 cm^{-1} ,3250 cm^{-1} & 3400 cm^{-1} were observed which may be due to aliphatic –CH- chain stretch, an aromatic stretch of –CH-, -NH- stretch and –OH- stretch respectively. The major peaks mentioned above confirms the structure of the PTX which confirms the identity of the drug. In Figure 5.36 (C), the peaks of secondary –NH stretch (3412.190), aromatic C-H stretch (2962.76), C=H aliphatic stretch (2922.25), C=O keto stretch (1732.13), C=O amide stretch (1624.40) & C=O stretch (1244.13) were present which confirmed the combination of both drugs. Further, the FTIR data of optimized formulation (B1, B2 & B3) had shown the absence of major peaks of drugs which confirms the encapsulation of the maximum drug inside the nanoparticles while they retained all the major peaks of the polymer as well as of surfactant used. Also, the presence of all major peaks of the components confirmed the compatibility of the excipients and the drug.

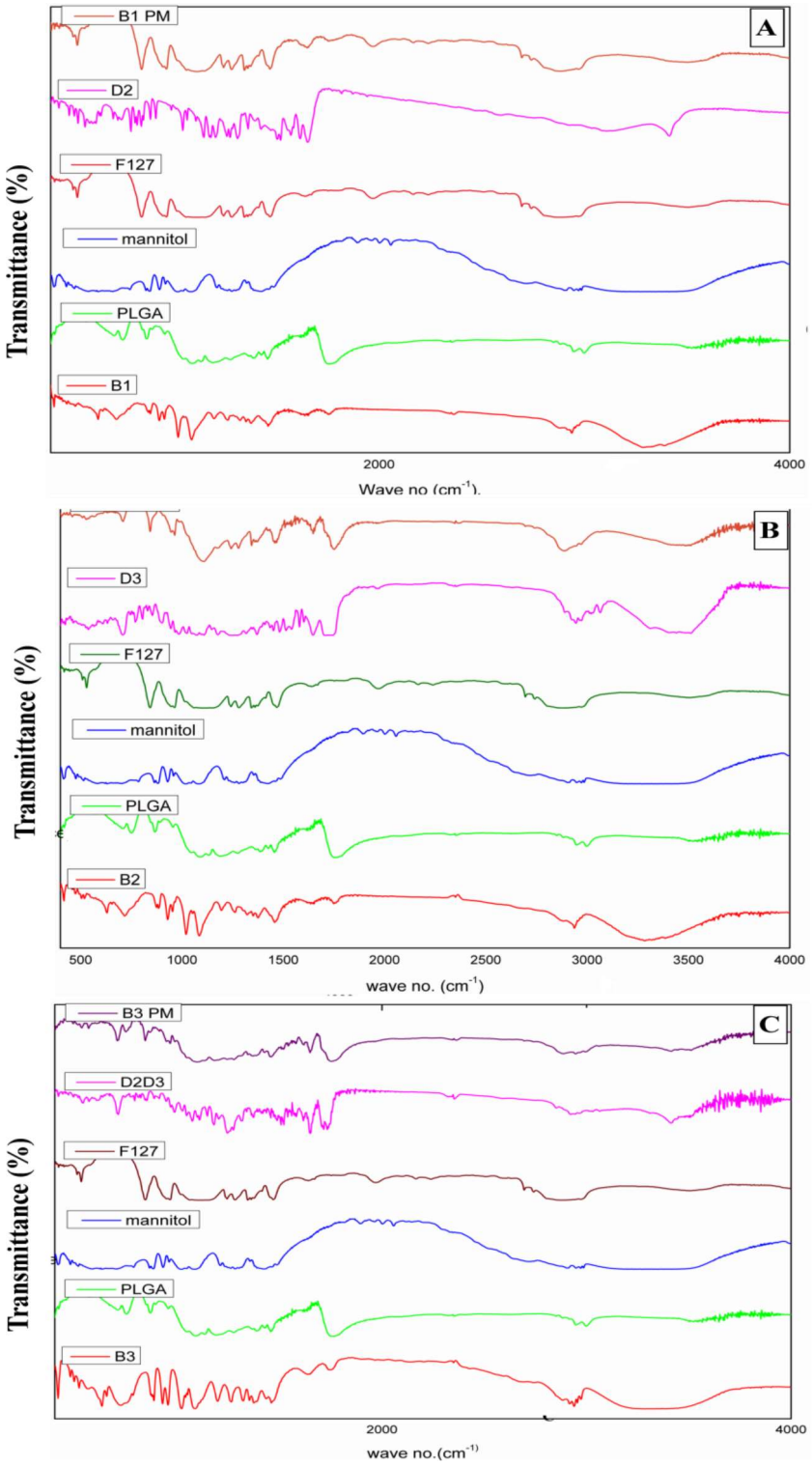

Figure 5.36: (A) Overlay FTIR spectra of Gen nanoparticles (B1), (B) Overlay FTIR spectra of PTX nanoparticles (B2), (C) Overlay FTIR spectra of combination nanoparticles (B3), Physical mixture (B1, B2 & B3 PM), Gen (D2),PTX (D3), Gen+ PTX (D2+D3) and all the excipients respectively.

Differential scanning calorimetry (DSC):

In DSC thermogram (Figure 5.37(A), Gen (D1) exhibit melting peak near 300˚C which is due to the actual melting of the molecule. In physical mixture (B1PM), melting peak of Gen was not visible while it contains the major peaks of surfactant (poloxamer 188). The DSC thermogram of PTX (D3) (Figure 5.37(B) showed an endothermic peak near 180- 220˚C which corresponds to the melting of the compound followed by an exothermic peak near 250˚C which corresponds to the degradation of the drug molecule. The physical mixture (B2 PM) showed the absence of melting and degradation peaks of PTX while showed the major peaks due to the presence of surfactant as well as polymer. In Figure 5.37(C), the DSC thermogram of D2+D3 showed one endothermic peak followed by exothermic peak near 210˚C which can be due to the PTX and one endothermic peak near 280˚C followed by the exothermic peak which is due to the presence of Gen. The physical mixture (B3 PM) retained all the peaks of polymer, surfactant and drugs. The absence of peaks of Gen and PTX in physical mixtures (B1, B2 & B3 PM) may be due to the solvation of the drugs respectively. Similarly, lyophilized formulations (B1, B2 & B3) showed the absence of major peaks of Gen & PTX whereas the sharp melting peak was present near 160˚C in all the spectra which was due to the presence of mannitol. Mannitol was added as cryoprotectant to the formulations during lyophilization. The peaks of the other excipients were present in the lyophilized formulation. The absence or reduction of peaks of drugs in the formulation can be attributed to the successful encapsulation of the drug molecule inside the nanoparticle formulations (44).

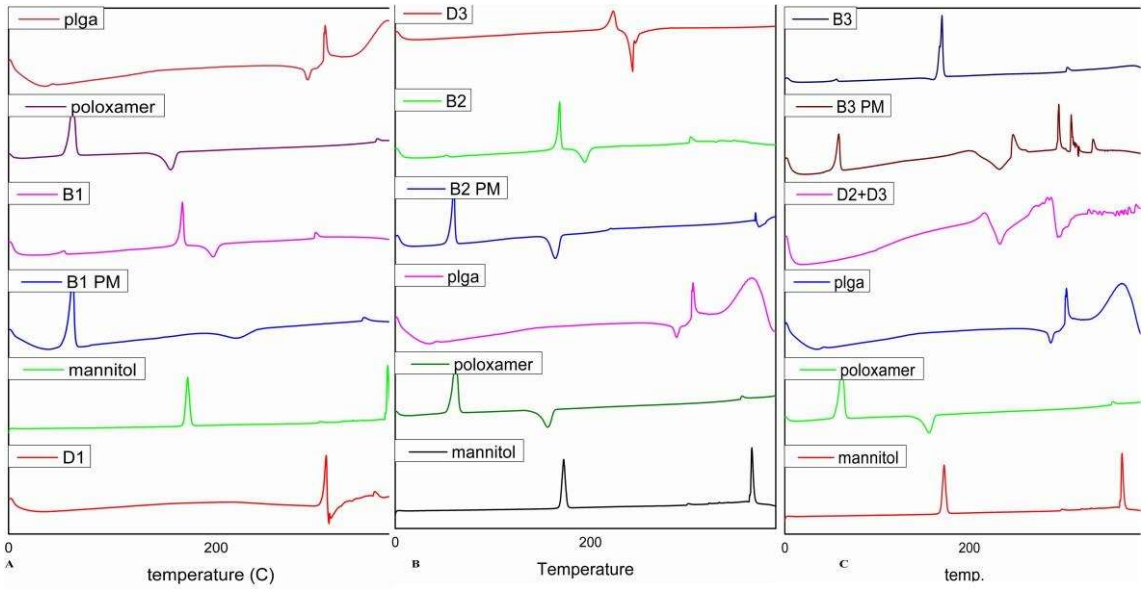

Figure 5.37: DSC thermograms of (A) Genistein (D1) and Gen loaded nanoparticles (B1). (B) Paclitaxel (D3) and PTX loaded nanoparticles (B2), (C) combination of both drugs (D2+D3) and their nanoparticles (B3), physical mixture (B1, B2, B3 PM) and all excipients.

Powder- X Ray Diffraction study (P-XRD):

The PXRD patterns of pure drug, polymer, surfactant, and the optimized formulation were examined during the study as shown in Figure 5.38. Genistein showed numerous peaks at Θ angle of approx 7˚, 9˚, 10˚, 11˚, 15˚& 20˚ and numerous minor peaks upto 30˚ (Figure 5.38 (A). PTX showed characteristic distinctive peaks at Θ angle of approx 5˚, 8˚, 15˚, 18˚& 20˚ and numerous minor peaks up to 35˚ (Figure 5.38(B). In Figure 5.38(C), D2+D3 (combination of PTX+Gen) retained all the major peaks of both drugs. The spectrum of PLGA showed a diffused broad peak indicating its amorphous nature. Also, poloxamer possessed two sharp peaks near 20 &27˚ approximately indicating the crystalline nature of the surfactant. The optimized lyophilized formulations (B1, B2 & B3 without mannitol) also showed broad diffused halo retaining the peaks of PLGA at

same diffraction angle. The diffraction pattern of B1, B2 & B3 had indicated that all characteristic intense peaks of PTX & Gen had abridged in their intensity and made a diffused broad halo which confirmed the physical state of drugs that had been converted from crystalline towards amorphous state (13).

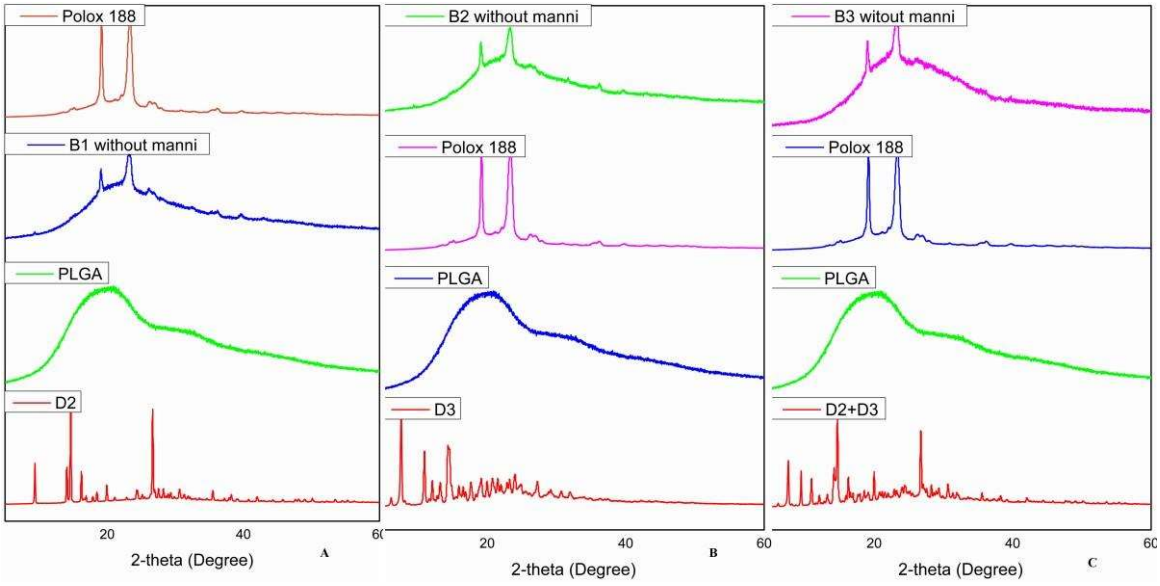

Figure 5.38: P-XRD spectra of (A) Genistein (D2) and Gen loaded nanoparticles (B1). (B) Paclitaxel (D3) and PTX loaded nanoparticles (B2), (C) combination of both drugs (D2+D3) and their nanoparticles (B3) and all excipients.

Particle size (PS), Polydistersity index (PDI), Zeta potential (ZP) & Entrapment efficiency (EE)

Particle size analyzer (Delsa Nano C) was used to calculate the three parameters (PS, PDI & ZP) which works on the phenomenon of Brownian motion, and light scattering whereas the value & charge of zeta potential are determined by the chemical nature of the drug, polymer, & most importantly on the nature of surfactant used. The values of PS, PDI & ZP of the optimized formulations are given in Table 5.23. The magnitude of the zeta potential charge was large enough to keep the particles apart and hence

confirms the stability of the formulation (11, 56, 59, 63, 64). Also, the negative charge of the nanoparticles will delay their protein binding and thereby results in longer circulation half-life of the nanoparticles. The PDI values of the formulations affirmed that the fabricated nanoparticles were of excellent nano range and the size was uniform throughout the formulation (65, 66). The entrapment efficiency shows that the optimized formulations can entrap sufficient amount of drug inside to release the appropriate amount of drug over an extended period of time.

Table 5.23: Particle Size, PDI, Zeta Potential & Entrapment Efficiency of optimized formulations.

Formulation	PS (nm)	PDI	ZP(mV)	EE (%)
B1	138.32±8.23	0.114±0.003	-19.71±1.19	96.7±2.35
B2	142.56±4.59	0.116±0.002	-20.36±2.36	94.34±3.43
B3	147.87±2.28	0.112±0.004	-21.86±3.11	93.27±2.19 (Gen, 94.51 for PTX)

Surface morphology studies:

The prepared formulations were observed under TEM & AFM to study the size as well as surface morphology of the prepared nanoparticles. The nanoparticles were found to be in the range of 130- 150 nm size throughout the image area as shown in Figure 5.39 (A-C) & 5.40 (A-C). The size observed under the microscope was also acquiescent with the particle size observed under particle size analyzer. The AFM image concluded the uniformity of surface of the nanoparticles.

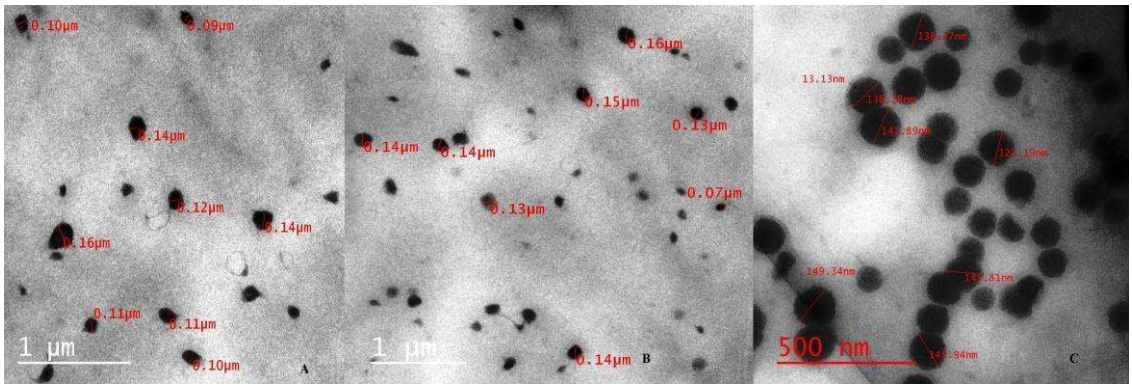

Figure 5.39 (A-C): Transmission electron microscopic images of optimized formulations (A- Gen nanoparticles, B- PTX nanoparticles & C- Gen+PTX nanoparticles)

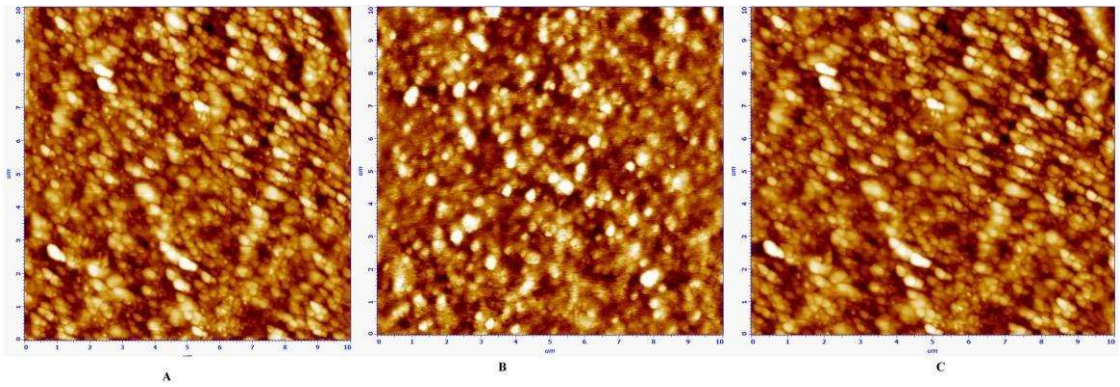

Figure 5.40 (A-C) Atomic force microscopic (AFM) images of optimized formulations (A- Gen nanoparticles, B- PTX nanoparticles & C- Gen+PTX nanoparticles)

Cumulative percentage drug release study:

In vitro release profiles of optimized formulations B1 & B2 in comparison to their respective pure drugs i.e. Gen and PTX are shown in Figure 5.41. 93% drug release was observed for PTX pure drug in 24 hours. The formulation showed minute amount of burst release which can be due to the lesser amount of free drug present. Moreover the

87% of the paclitaxel was released from B2 formulation and 85% of paclitaxel was released from combination formulation B3 in 96 hrs (Figure 5.42). The slower release of the drug from the nanoparticle system can be due to the presence of polymeric matrix which provides the barrier to curtail the immobilization of the drug from the polymer system and also the lipophilic nature of the drug could be the reason for slower release. PLGA is a bulk eroding polymer and hydrolytic cleavage of ester bonds initiate the attrition mechanism of the polymer. The drug release from the polymer occurs because of diffusion of drug as well as degradation of polymer matrix. Biphasic release pattern was observed for the release of drugs from the nanoparticle system. The unentrapped drug present in the formulation was responsible for the burst release of the drug during the initial period (47) while the entrapped drug was responsible for the delayed release of the formulation. Approximately 58% release of the Gen was observed from B1 formulation & 56% of Gen was released from combination formulation B3 till the end of 96 hrs (Figure 5.42), whereas the drug release of Gen pure drug was about 22% at the end of 24 hrs. We also analyzed the release mechanism of both formulations by substituting the release profile and time data to various kinetics models their correlation coefficient and release exponent values are mentioned in Table 5.24. From the values of R^2, it was concluded that release kinetics of nanoparticles followed Higuchi model of release kinetics and the fickian diffusion based release mechanism was followed as evidenced by release exponent value of Korsmeyer Peppas model which was found to be 0.306 for B2 ,0.435 for B1 & (0.446, 326) for B3 ($n<0.5$ for fickian diffusion controlled mechanism)(59).

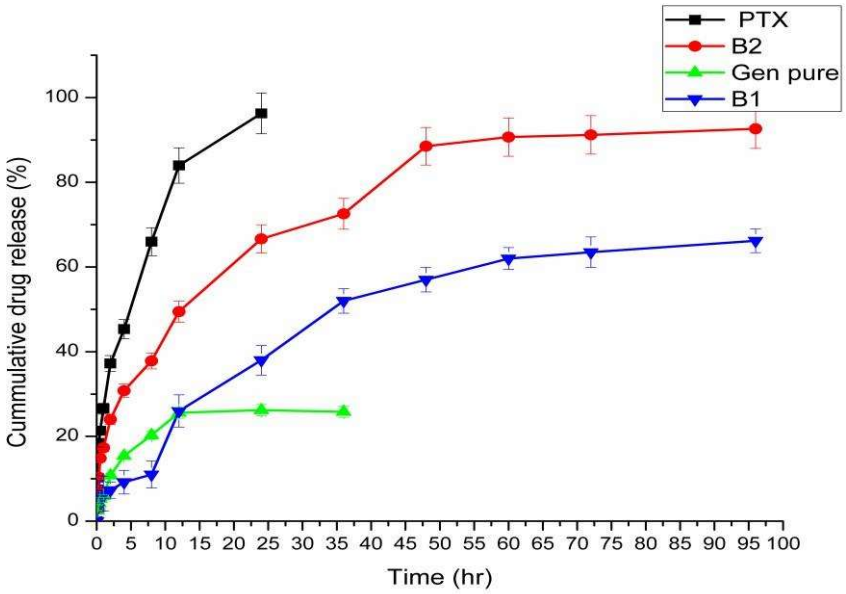

Figure 5.41: In vitro drug release profile of B1 & B2 in comparison to their pure drugs in phosphate buffer saline pH 7.4. Vertical bars represent S.D, n=3.

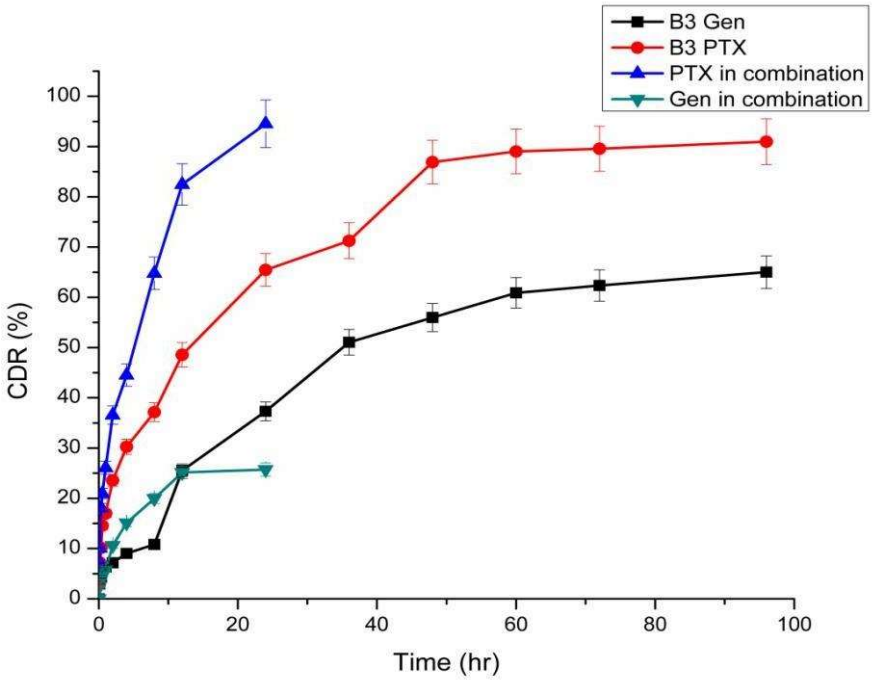

Figure 5.42: In vitro drug release profile of B3 in comparison to its pure drug combination in phosphate buffer saline pH 7.4. Vertical bars represent S.D, n=3.

Table 5.24: Correlation coefficients & release exponent values for various release kinetics models for in vitro release kinetic from optimized nanoparticle formulation

Release Kinetics Models	B1(Gen)		B2(PTX)	
	Correlation coefficient (R^2)	Release exponent (n)	Correlation coefficient (R^2)	Release exponent (n)
Zero Order	0.7368	-	0.8543	-
First Order	0.9060	-	0.9292	-
Higuchi model	0.9643	-	0.9838	-
Korsemeyer-Peppas model	0.9496	0.435	0.9672	0.306
Release Kinetics Models	**B3 (Gen)**		**B3 (PTX)**	
	Correlation coefficient (R^2)	**Release exponent (n)**	**Correlation coefficient (R^2)**	**Release exponent (n)**
Zero Order	0.7745	-	0.8489	-
First Order	0.9142	-	0.9256	-
Higuchi model	0.9754	-	0.9801	-
Korsemeyer-Peppas model	0.9523	0.446	0.9663	0.326

Stability Studies:

To calculate the shelf life of the formulations, stability studies were performed at different conditions of temperature and humidity. Shelf life was calculated based on percentage entrapment efficiency of the formulations which was calculated at different time periods throughout the study. Minitab® version 7 was employed to construct the shelf life graphs (Figure 5.43). Particle size, Zeta potential, PDI were also determined in comparison to fresh samples, and all these traits were found to be non-significantly different ($p>0.05$) at these conditions. The shelf life observed was about 12.2, 12.5 &12.7 months for B1, B2 & B3 respectively at all storage conditions of temperature and humidity. Thus it was concluded that PLGA based NLCs can be stored for sufficient period of time (55).

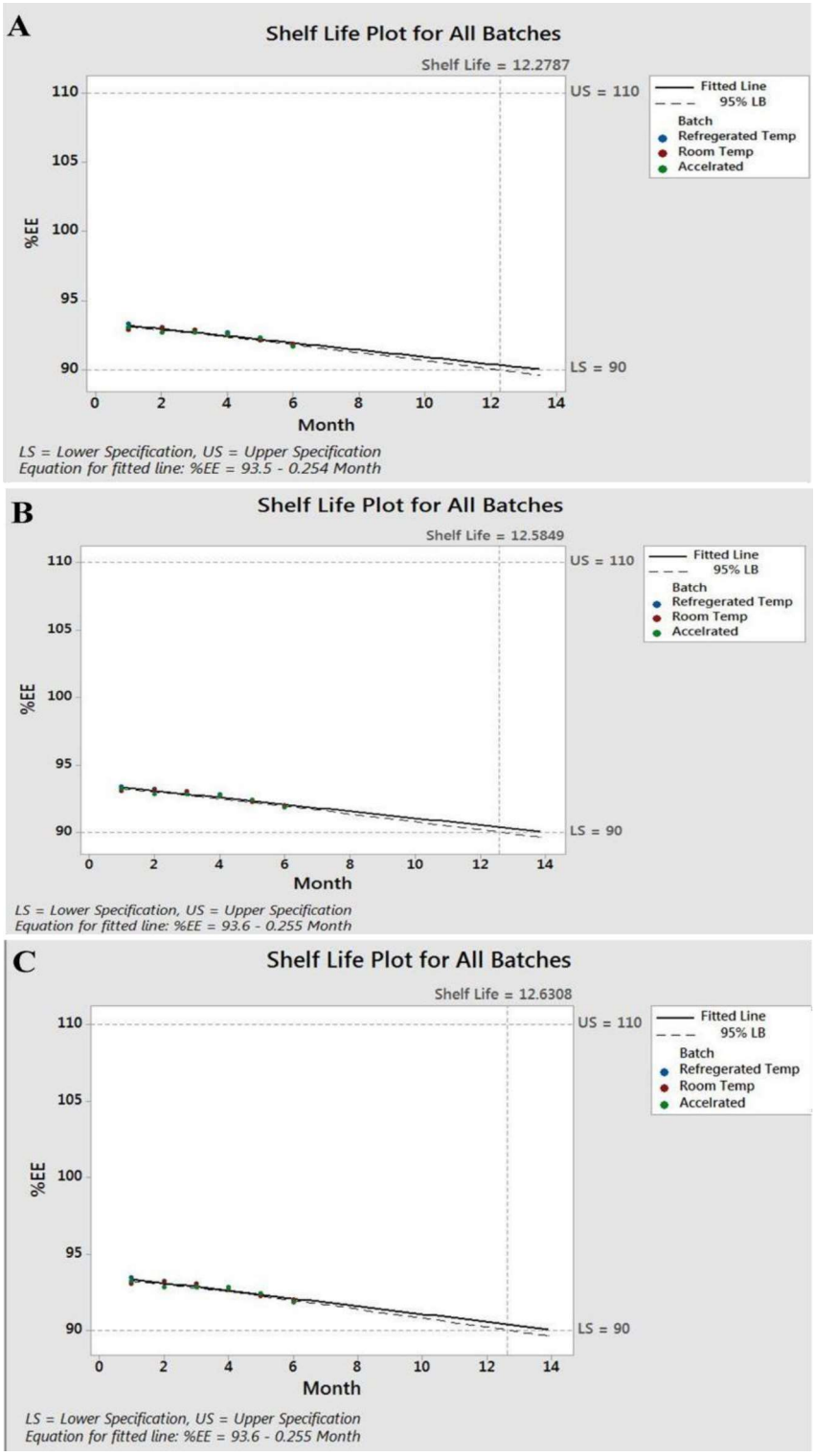

Figure 5.43: Shelf life estimation of optimized batches of polymeric nanoparticles (B1, B2 & B3) at various storage conditions.

Haemocompatibility Studies:

Heamolysis:

Heamolysis seems to be the most important role playing factor for the evaluating the ability of the formulation for intravenous administration as the excipients like polymers and surfactants can cause haemolysis of the blood cells. Therefore, the haemolytic potential of pure drug, placebo as well as optimized formulation was verified at different time intervals at two different concentrations. According to Brazilian standards, the limit for spontaneous haemolysis should not be more than 1%. Any of the compound or formulation, intended for i.v use should not cause more than 1% of haemolysis of erythrocytes (67). In our experiment, the samples did not cause significant heamolysis of the blood at lower (10 µg/ml) concentration when incubated for 8 hrs but at 100 µg/ml, the limit was slightly excedded for formulations, pure drugs as well as for placebo during the last hour of the sampling which could be due to interaction of the blood cells with the polymer and the surfactant present (46), Fig 5.44 (A-C). The surfactant at a higher concentration can penetrate the cell membrane and solubilize the lipids present there. When membrane lipids are exposed to the higher concentrations of the formulation, dissolution of the membrane lipids get starts which causes destruction of the erythrocytes (56). This hypothesis would be sufficient to explain the reason behind exceeding heamolysis limit by the nanoformulations.

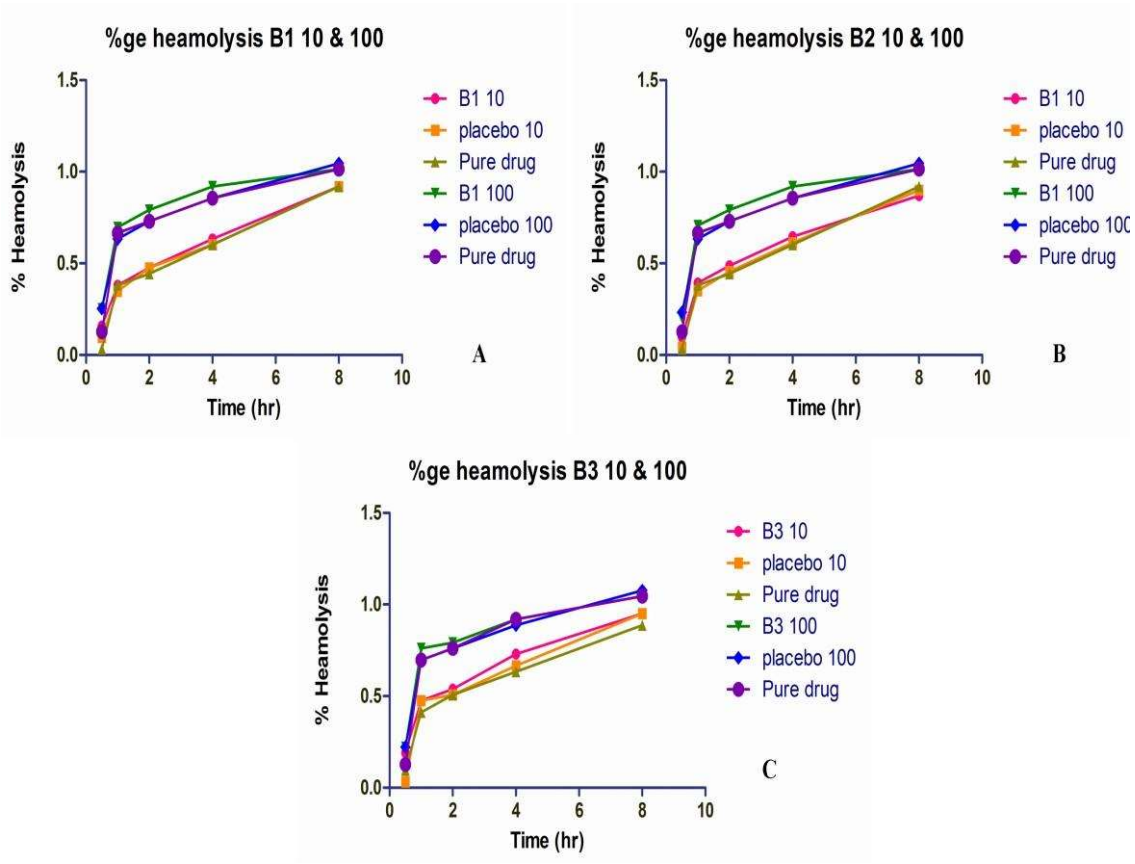

Figure 5.44: Heamolysis profiles of B1, B2 & B3 nanoparticles, placebo and their pure drugs at different concentrations.

Platelet aggregation test:

Platelet aggregation upon addition of tests formulation to the citrated whole blood is also an integral part of testing the haemocompatibility of formulations for i.v use. To evaluate the aggregation in platelets, formulations, pure drugs, placebo formulation and PBS were added at 10 & 100 µg/ml in the citrated whole blood and the smears were observed under immersion lens of optical microscope. Also, the no. of platelets were counted by haematological counter. Aggregation of platelets is associated with major problems viz. thrombocytopenia, heart attack; hemorrhage etc. which can lead to the death of the patient so should be evaluated at during formulation studies. The

nonsignificant difference ($p>0.05$) in platelet count was observed for all the samples in comparison to PBS at 10 µg/ml concentrations while at 100 µg/ml, Pure drug suspensions showed a significant decrease ($p<0.05$) in number of platelets in comparison to PBS and all other groups (Figure 5.45). The decrease in number of platelets at higher concentrations by the pure drug suspensions can be explained on the basis of potential of paclitaxel in causing neutropenia and genistein‟s anticancer effect after administration. In addition to the platelet count, platelet aggregation was also observed by optical light microscopy, and platelets were indicated by arrows in the photographs in Figure 5.46. Supportively, no platelet aggregation was observed of any of the samples which authenticate the nontoxicity of developed formulation for intravenous use (47).

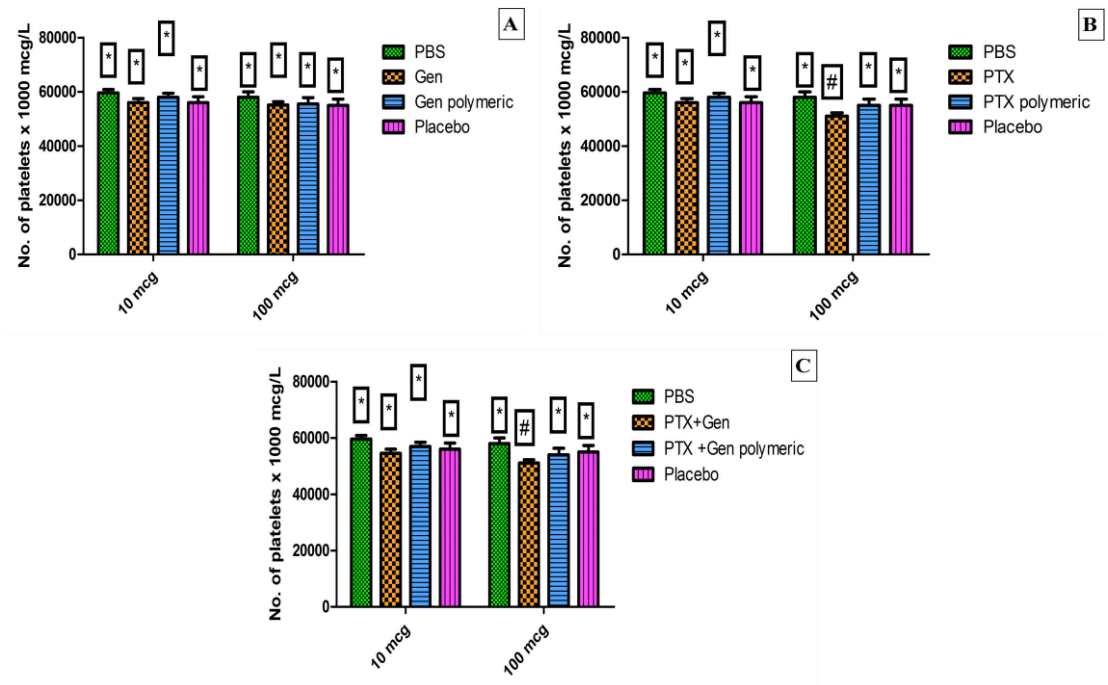

Figure 5.45: No. of platelets after addition of (A) B1, Gen (B) B2, PTX (C) B3, Gen+PTX; PBS & Placebo at 10 & 100 µg/ml. Vertical bars represent Mean±SEM, n=3. *Data is non significantly different at $p>0.05$ from PBS (negative control). # Data was significantly different at $p<0.05$ from PBS.

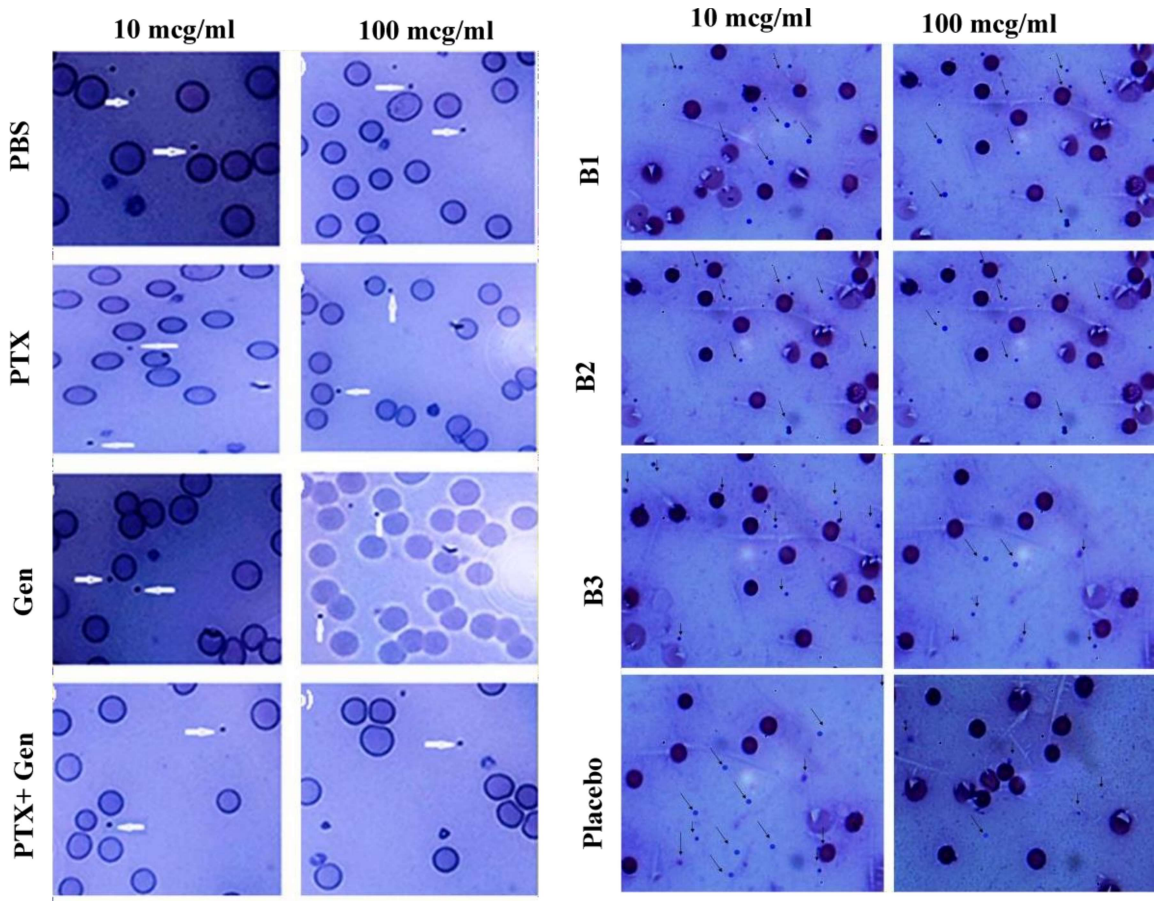

Figure 5.46: Platelet aggregation optical microscopy images of Leishman's stained whole blood samples after treatment with PBS at 10 & 100 µg/ml, pure drugs (PTX, Gen & PTX+Gen) at 10 & 100 µg/ml, Placebo formulation at 10 & 100 µg/ml & optimized formulations (B1, B2 & B3) at 10 & 100 µg/ml. Images were captured at magnification of 100x.

In vitro cytotoxicity study:

In vitro cell line studies were performed on PA-1 cell lines. 100 µM solutions of Gen, PTX, Gen+PTX, B1, B2 & B3 were prepared in distilled water as stock solutions. From the stock, dilutions were made in the range 10 to 50 µg mL^{-1}. Cells in conc.1 $\times 10^4$ cells per well were incubated in 96 well plated for 48 h and then treated with the prepared dilutions. Placebo of the formulation was taken as positive control during the studies and normal saline as negative control. Results are shown in Figure 5.47. Among PTX

and Gen, PTX was more effective in controlling the cell growth at all concentrations ($p<0.05$). B2 formulation was more effective in controlling cell growth then B1 at higher concentrations while at lower concentration, both the formulations were equally effective ($p> 0.05$). At higher concentrations, the combination of drugs was equally effective to PTX in controlling the cell growth at $p>0.001$, similarly the combination formulation (B3) was also found to have equal cytotoxic potential to the PTXNLC (B2) at higher concentrations ($p>0.0001$).

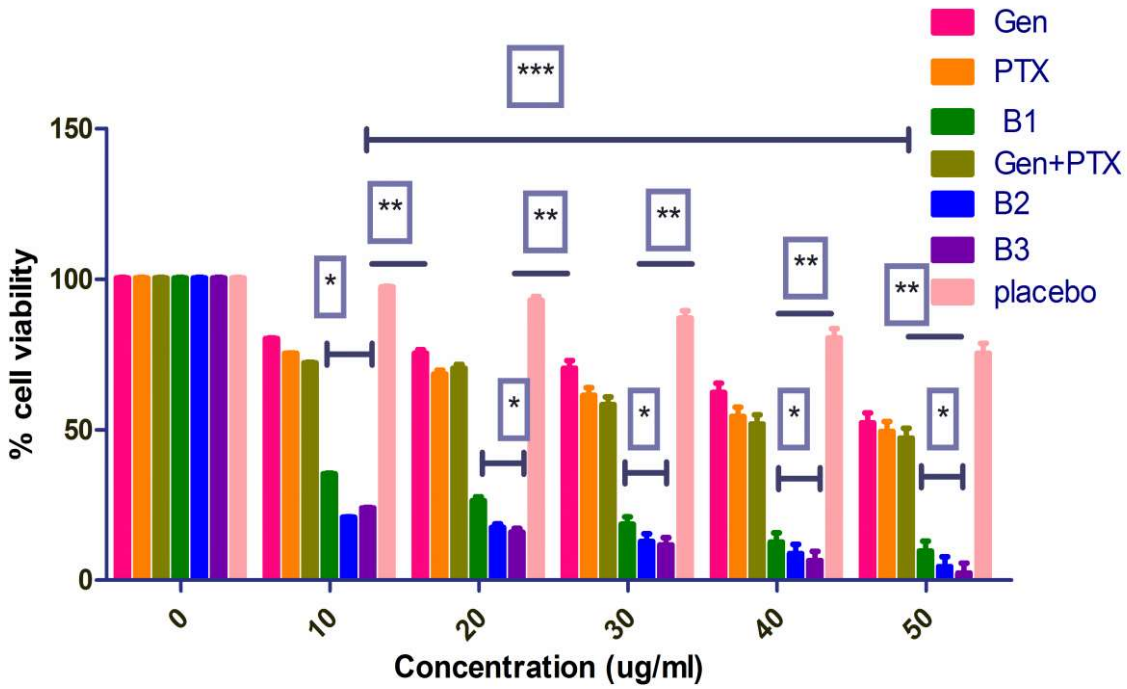

Figure 5.47: % cell viability of pure drugs (PTX, Gen & PTX+Gen), optimized formulations (B1, B2 & B3) & placebo at different concentrations. Results were analyzed by two way ANOVA followed by Bonferroni posthoc test; *: when compared with pure Gen at $p< 0.05$, **: when compared with pure PTX $p< 0.001$, *: when compared with pure drug combination of Gen+PTX $p< 0.0001$; Values are expressed as mean± SEM, n=3.**

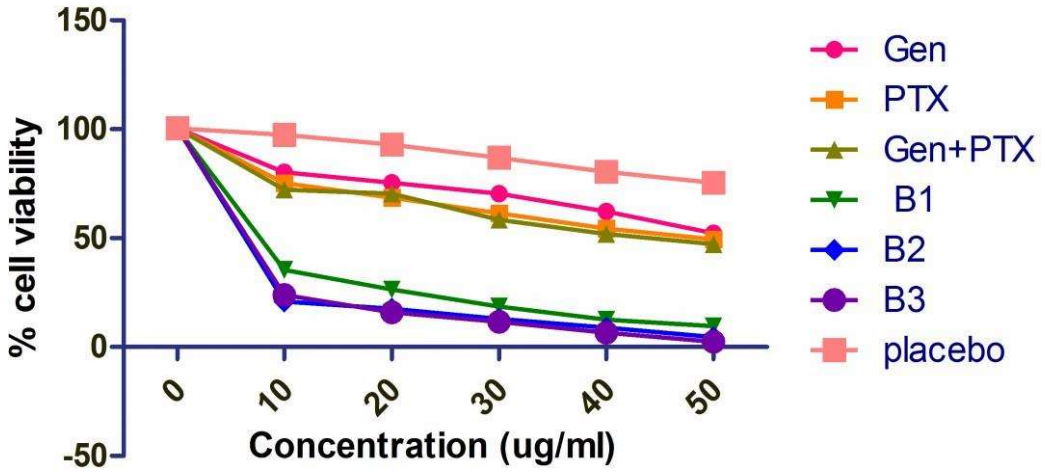

Figure 5.48: Scatter plot for the calculation of IC_{50} value.

IC_{50} values were also calculated by using curve fitting method. IC50 values for pure Gen, PTX, Gen+PTX & formulations B1, B2 & B3 were 61.2, 55.4, 50.8, 7.92, 5.44 & 4.61µM respectively. IC_{50} of B1 was reduced to 7.6 fold as compared to pure Gen. Similarly, IC50 of B2 was reduced to 10.23 fold then pure PTX and IC50 of B3 was 11.2 fold lower than combination of pure drugs. Enhanced cytotoxicity of the nanoparticles over pure drugs can be due to the enhanced cellular uptake of the nanoparticles by reticuloendothelial system (RES). Free drug crosses the cell membrane through diffusion whereas nanoparticles were taken by cells through special internalization pathway and releases the drug in a systematic manner. Cytotoxicity of the combination (B3) was almost equivalent to the individual PTX which concludes that combination of PTX and Gen nanoparticles can be used for the treatment of ovarian cancer in place of Pure PTX with lesser side effects to the patients.

Pharmacokinetic study:

Pharmacokinetics study was performed to estimate the fate of the administered drug in the form of nanoparticles and as pure drug via intravenous route. Plasma drug concentrations in rat plasma at different time intervals were measured up to 96 hrs. The plasma drug concentration vs. time profiles are shown in Figures 5.49 & 5.50 and their corresponding pharmacokinetic parameters are shown in Table 5.25. Plasma drug concentration vs. time profile data of all the samples is given in Tables 5.26 & 5.27. Pharmacokinetic analysis was performed by using PK solver add in of Microsoft excel. From the Figure 5.49, it can be seen that mean plasma concentrations decreases biexponentially in all the groups. Initially the mean plasma concentration was higher for the group treated with PTX pure (alone as well as in pure drug combination), but it was rapidly eliminated from the circulation. Encapsulation of PTX (A2 & A3) in polymeric matrix however, retarded the release of the drug for prolonged periods of time and higher drug levels were maintained for longer duration of time. Similar behavior was observed for Gen pure (alone as well as in combination) in comparison to its corresponding formulations B1& B3, but the plasma drug concentration of pure Gen was lower as compared to pure PTX due to the higher lipid solubility of the Gen. Prolonged circulation was further confirmed by 3.3 fold increase in AUC for B1 & 3.21 fold increase in AUC for B2 when compared with Gen pure and PTX pure drug respectively. Elimination half life was also improved significantly ($p<0.05$) as compared to pure drugs. For B3 formulation, AUC was enhanced by 3.1 folds for Gen and 3.5 folds for PTX when compared with the respective drugs in pure drug combination & $t_{1/2}$ was increased significantly ($p<0.05$) as compared to their respective pure drugs in

combination. Mechanism behind these observations was the prolonged release provided by encapsulation of drugs in polymer matrix which retarded the clearance as the drug from the body. Drug releases from PLGA matrix for prolonged period of time hence decreased the amount of free drug present in the systemic circulation (58). This observation suggests that polymeric nanoparticles incorporated with drug molecules could be a preferred tool for the prolonged systemic circulation. Overall circulation behavior of the drug was vastly improved through encapsulation of the drugs inside the polymeric matrix.

Table 5.25: Pharmacokinetic parameters of pure drugs (Gen, PTX & Gen+PTX) and their corresponding polymeric nanoparticles (B1, B2 & B3)

Groups	C_{max} (ng/ml)	AUC ({ng/ml}*hr)	$t_{1/2}$ (hr)
Pure PTX	5400.03	31666.83	7.07
Pure Gen	4300.02	21111.22	6.89
Pure Gen in Gen+PTX	3823.09	24314.76	8.5
Pure PTX in Gen+PTX	5600.23	22810.87	4.8
Gen in B1	4132.16	69607.73	85.30
PTX in B2	5848.34	104411.60	74.37
Gen in B3	2600.33	60978.22	92.5
PTX in B3	3421.97	72557.29	122.09

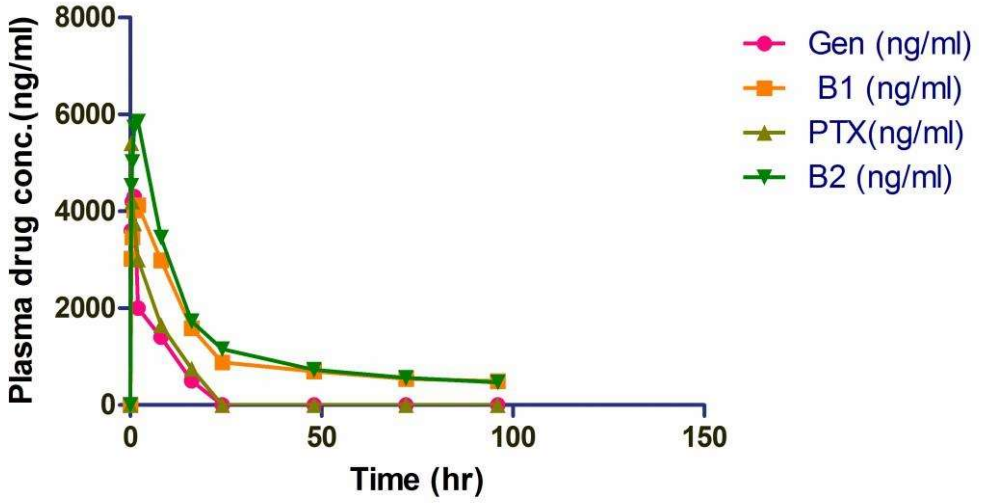

Figure 5.49: Comparative plasma drug concentration vs. time profile of Gen, PTX, B1 and B2 after intravenous administration. Dose administered was 10 mg/kg. Each data point represents mean ± SEM, at $p<0.05$.

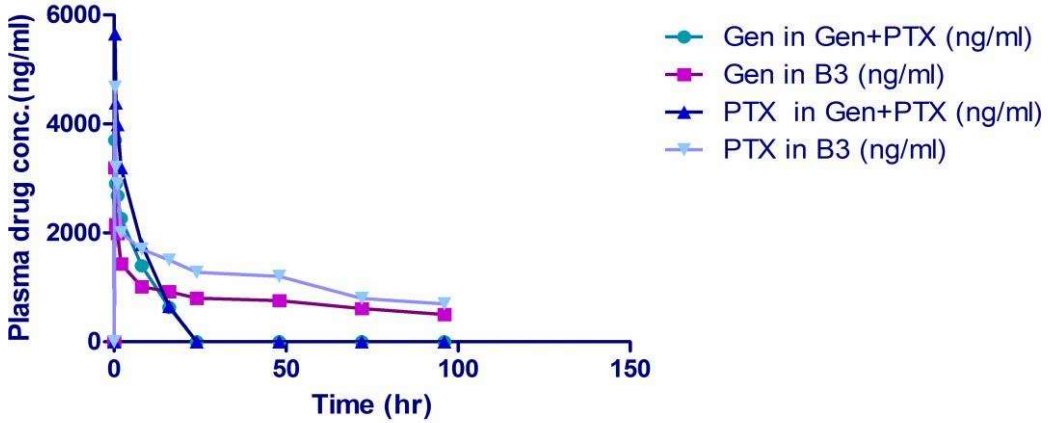

Figure 5.50: Comparative plasma drug concentration vs. time profile of Gen, PTX, in pure drug combination and in combination formulation B3 after intravenous administration. Dose administered was 10 mg/kg. Each data point represents mean ± SEM, at $p<0.05$.

Table 5.26: Plasma drug concentration (PDC) and time data of pure PTX, Gen and their corresponding formulations (B1 & B2)

Time(hr)	PDC (PTX)	PDC B2	PDC (Gen)	PDC B1
0.00	0.00	0.00	0.00	0.00
0.25	5400.03	4533.00	3600.02	3022.76
0.50	4200.07	5018.00	4200.00	3465.88
1.00	3750.00	5730.00	4300.00	4020.70
2.00	3000.15	5848.24	2000.10	4132.16
8.00	1651.09	3456.56	1400.00	2987.34
16.00	750.84	1731.10	500.56	1587.40
24.00	0.00	1156.68	0.00	881.12
48.00	0.00	732.00	0.00	693.60
72.00	0.00	560.00	0.00	540.87
96.00	0.00	514.79	0.00	372.19

Table 5.27: Plasma drug concentration (PDC) and time data of pure PTX , Gen in pure drug combination and in combination formulation (B3)

Time (hr)	PDC Gen PTX+Gen	PDC Gen B3	PDCPTX PTX+Gen	PDC PTX B3
0.00	0.00	0.00	0.00	0.00
0.25	3823.65	3198.37	5600.03	4676.77
0.50	3000.98	2154.87	4400.00	3200.15
1.00	2700.43	1987.11	3950.00	2900.95
2.00	2200.23	1432.72	3100.00	2000.04

8.00	1300.65	1011.98	200.00	1700.08
16.00	700.24	921.64	900.00	1500.70
24.00	0.00	801.19	0.00	1278.19
48.00	0.00	756.15	0.00	1200.65
72.00	0.00	611.34	0.00	798.98
96.00	0.00	501.76	0.00	698.15

In vivo biochemical estimations:

In vivo biochemical estimations were performed in order to evaluate the blood serum parameters in respect of liver toxicity (SGOT, SGPT, ALP & Total Billirubin) and Neutropenia (Absolute Neutrophil Count (ANC) after the administration of prepared formulations by i.v route at a dose of 10 mg/kg. Pure saline (0.9% NaCl) was kept as control and pure drugs were also evaluated for their comparisons with the respective formulations. From the results as shown in Figure 5.51, it was concluded that PTX increased the level of ALP, AST and TBIL and decreased the level of ALT which cause liver damage at raised levels. Decrease in neutrophil count was also observed by PTX & PTX+Gen which were less pronounced with B2 and least with B3. Significant difference was observed when control was compared with B2. No significant difference was observed when control was compared with B3. Entrapment of drug (PTX) in polymer matrix decreased the toxic effects caused by pure drug but the masking of toxicity was not upto the mark which was obtained when Gen was incorporated along with PTX in a ratio of 1:5 (Gen:PTX). So, the ratiometric combinationof phytoestrogen

along with chemotherapeutic semi synthetic drug had been proved to be safe and equally effective medication for the treatment of ovarian cancer.

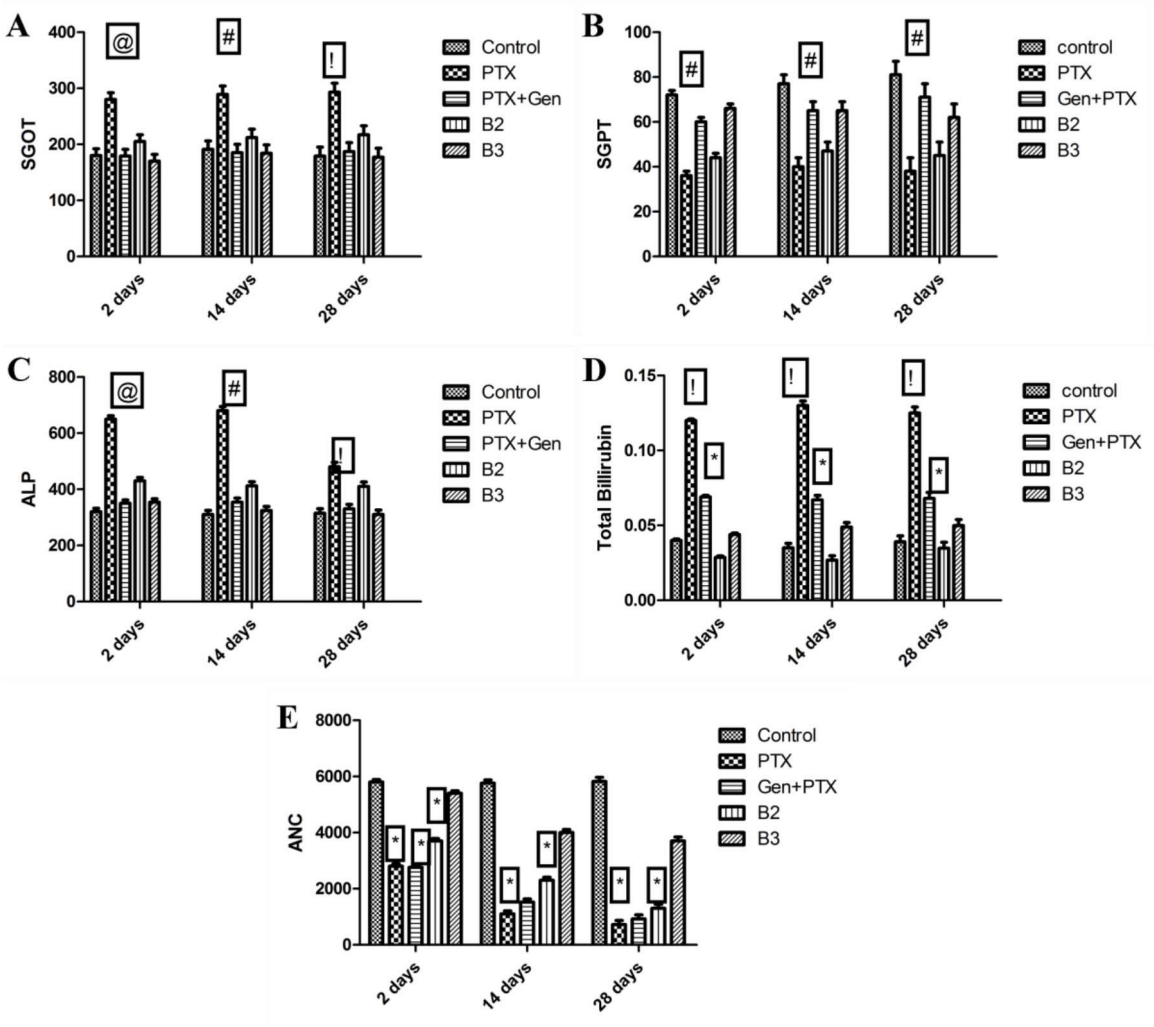

Figure 5.51. Blood serum levels of (A) Aspartate aminotransferase (AST or SGOT) (B) alkaline phosphatase (ALP), (C) alanine transaminase (ALT or SGPT) (D) Total billirubin and (E) absolute neutrophil count (ANC) after the administration of A2 & A3 in comparison to their respective pure drugs at a dose of 10mg/kg. 0.9% saline act as control. Each data point represents mean ± SEM, @ at p< 0.0001, # at p< 0.001, ! at p<0.05 and * at p< 0.0001 as compared to control.

In vivo anticancer study:

In vivo anticancer study was performed in Balb/c mice of age about 8-10 weeks by injecting ID-8 murine epithelial ovarian cell line. A significant decrease in % tumour growth, tumor volume & relative tumour volume was observed for B3 formulation in comparison to combination pure drug, however, the % tumour growth for the group treated with standard (doxorubicin, i.v) was almost same to the group treated with formulation at different time intervals (Figures 5.52-5.54). All the groups showed 100% survival during the study and their body weight at the end of the study was also found in the desired range in comparison with initial weight. Thus the combination of synthetic drug along with phytoconstituent provides the synergistic effect for the treatment of ovarian cancer and offered least toxicity to the subjects.

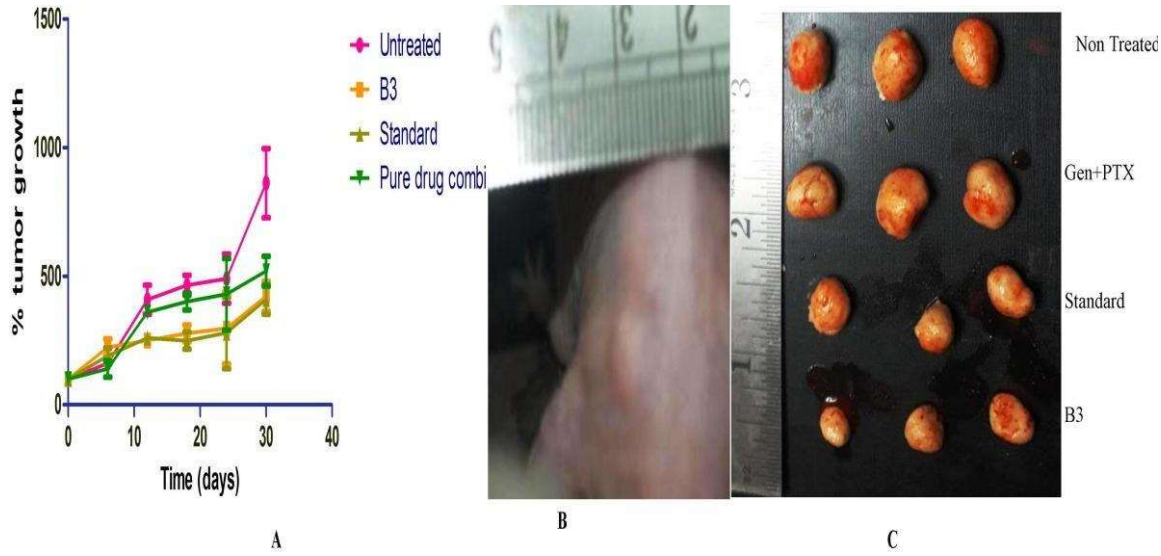

Figure 5.52: (A) Graphical representation of % tumor growth vs. time (days) with treatments administered i.v. on the days mentioned on the graph. Error bars represent SEM, n=3, p value <0.001. (B) Representative image of tumor (c) Images of whole excised tumors for different test groups.

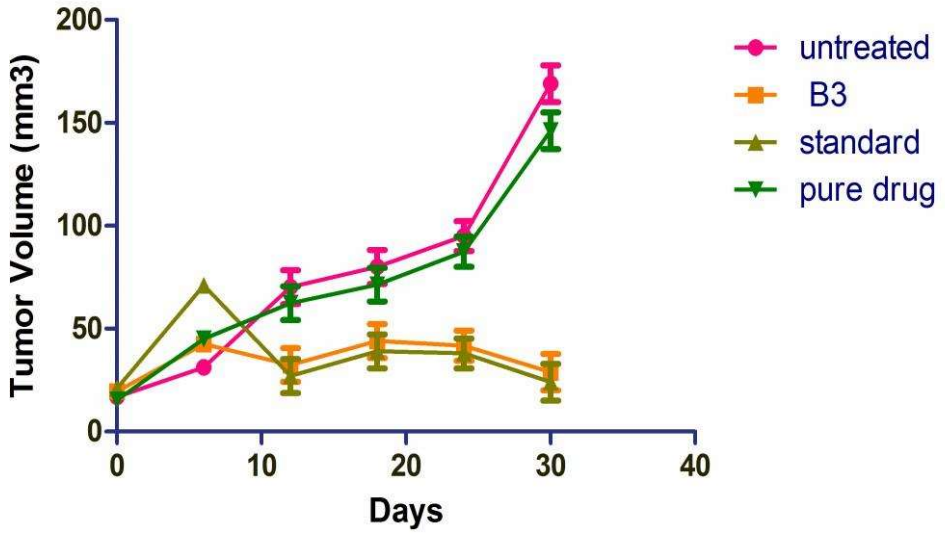

Figure 5.53: Tumor volume of combination formulation; B3 in comparison to its pure drug combination. Results were analyzed by two way ANOVA followed by Bonferroni posthoc test; (@p< 0.001) & (# p<0.0001).

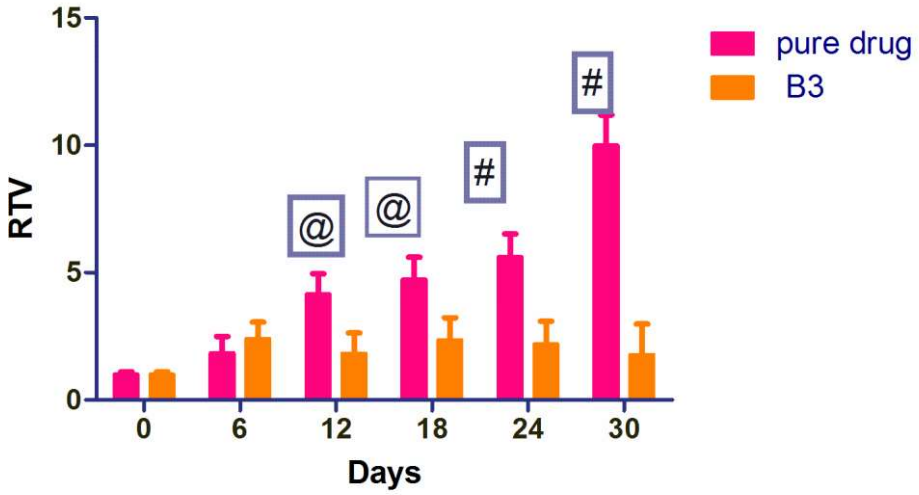

Figure 5.54: Relative tumor growth rate of combination formulation; B3 in comparison to its pure drug combination. Results were analyzed by two way ANOVA followed by Bonferroni posthoc test ; (@p< 0.001) & (# p<0.0001).